e-Prime - Advances in Electrical Engineering, Electronics and Energy 4 (2023) 100140

Contents lists available at ScienceDirect

e-Prime - Advances in Electrical Engineering, Electronics and Energy

journal homepage: www.elsevier.com/locate/prime

A comparative analysis of the performance of multiple meta-heuristic algorithms in sizing hybrid energy systems connected to an unreliable grid

Saheed Ayodeji Adetoro [a,*], Lanre Olatomiwa [a,c], Jacob Tsado [a], Solomon Musa Dauda [b]

[a] Department of Electrical and Electronics Engineering, Federal University of Technology Minna, PMB 65, Minna, Nigeria
[b] Department of Agricultural and Bioresources Engineering, Federal University of Technology Minna, PMB 65, Minna, Nigeria
[c] Department of Electrical and Electronic Engineering Science, University of Johannesburg, Johannesburg 2006, South Africa

ARTICLE INFO

Keywords:
Hybrid renewable energy system
HOMER Pro
Meta-heuristic algorithms
Unreliable grid
Biogas generator
Net present cost
Levelised cost of energy

ABSTRACT

The availability of affordable and reliable power supply fosters social and economic growth and raises the standard of living. In most developing nations, there is a considerable gap between energy supply and demand, often resulting in load shedding and blackouts. Integrating two or more renewable power sources is a potential solution for the inconsistent nature of renewable energy, thereby supplying clean and sustainable electricity. However, proper component sizing and operation planning for different system components are necessary for a reliable and cost-effective system. This paper compares the performance of three widely used optimisation techniques (Artificial Bee Colony (ABC), Genetic Algorithm (GA), and Particle Swarm Optimisation (PSO)) in determining the size of a hybrid renewable energy system (HRES) with the lowest levelised cost of energy (LCOE) to meet the energy needs of a dairy farm in a rural settlement. PSO is observed to be the best-performed algorithm proposing a system with an LCOE of $0.162 per kWh, a net present cost (NPC) of 2.05 million dollars and a payback period of 5 years and 7 months when compared with the existing power system. The proposed HRES is determined to reduce annual diesel usage by 96%. Therefore, significantly decreasing greenhouse gas (GHG) emissions. The PSO algorithm performs satisfactorily in terms of results and convergence time compared to the results from commercially available hybrid optimisation software (HOMER Pro).

1. Introduction

With the ever-increasing world population, there has been continuous industrial and household energy growth. Nigeria's energy crisis has become the main impediment to economic growth. Despite several attempts, like most sub-Saharan African countries, Nigeria needs a more reliable energy supply [1]. Nigeria's outdated electricity infrastructure is unable to consistently fulfil customers' ever-increasing demand, resulting in regular load shedding. According to World Bank data [2], Sub-Saharan Africa is home to 90% of the 650 million people who will still be without electricity in 2030. Industrial operations require constant supply, and even minor disruptions might cost millions of dollars. During power outages, most affected customers in the industrial and commercial sectors turn on diesel generators (DG) as a dependable backup source of electricity. DG has a lower initial capital cost per kWh than most renewable energy sources (RESs). Hence, DG is the most affordable option to meet the energy demand during grid outages. However, since diesel generators require expensive fuel, their operating expenses are substantially greater. Therefore, RESs are cost-effective in the long run [3].

Nigeria, a tropical country, has ample sunshine and agricultural activity. Hence, the country has abundant renewable energy resources (RERs), including solar, biomass, hydropower, and wind (in the coastal regions). There is a good potential for harnessing these RERs to supplement the national grid's energy supply and satisfy the country's urban and rural electricity demand [4,5]. Therefore, HRESs have received significant attention in most recent studies. However, the power production of energy systems such as solar photovoltaics (PV) or wind turbines (WT) is dependent on the availability of resources such as sunshine or wind. As a result, the nature of the power output is intermittent; hence, it must be used when available or stored [6]. The reliability of renewable energy systems can be improved by combining different yet complementary RESs, sometimes paired with a dispatchable energy source, such as a diesel, gasoline, or biogas generator, as a backup. According to research by Sanni et al. [4], a dispatchable biogas generator (BG) fuelled by methane from organic waste obtained

* Corresponding author.
E-mail address: adetoroayo@gmail.com (S.A. Adetoro).

https://doi.org/10.1016/j.prime.2023.100140
Received 1 January 2023; Received in revised form 5 February 2023; Accepted 10 March 2023
Available online 12 March 2023

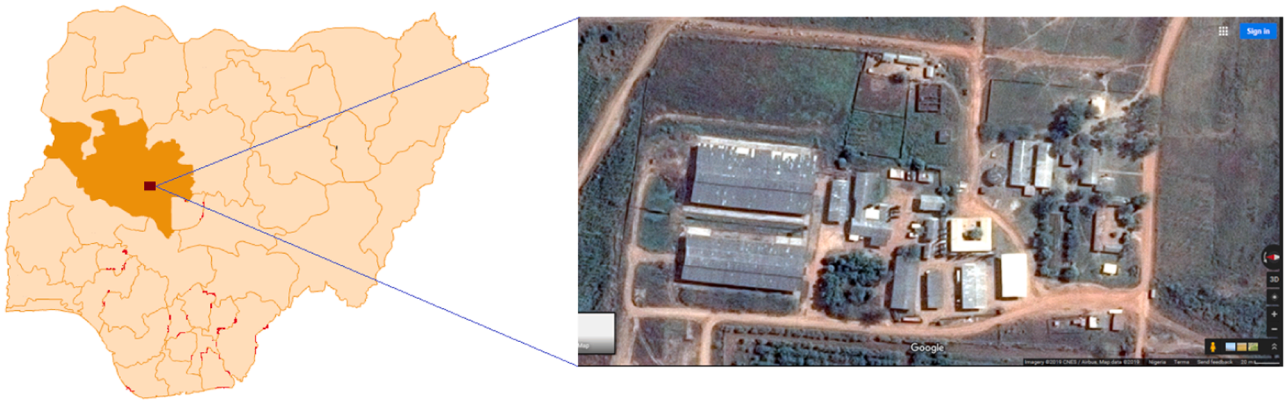

Fig. 1. Aerial view of Maizube Farm, Sabon Daga, Niger State, Nigeria. (Source: earth.google.com).

from a central slaughterhouse in Ado-Ekiti, Nigeria, can be used to improve the reliability of HRES connected to an unreliability grid.

With proper component sizing and an efficient energy dispatch strategy, an HRES can be a sustainable, cost-effective, and reliable alternative to meet the energy demands of developing countries. Although using a DG in a hybrid system presents financial and environmental issues, it may be necessary to incorporate it to improve the reliability of an off-grid HRES or in a case where the grid is unreliable. DG can also offset the peak demand in a location with a low power factor, improving the capacity factor of RESs. In some cases, HRES may require some sort of energy storage, particularly in off-grid systems, to absorb excess renewable energy. A battery bank is the most popular storage technique. However, supercapacitor and fuel cell technology have also been adopted in recent studies to capture surplus renewable energy [7,8]. Akinyele et al. [3] proposed the electrification of 100 off-grid homes in Nigeria utilising mini-hydro, solar PV, and diesel generators. The author introduced technological, environmental, economic, and policy (TEEP) analytical procedures in the study. The technical analysis of the study considers component sizing, energy production, unmet load demand, and loss of power probability; the environmental portion evaluates the emissions generated by the generator relative to when only a diesel-based generator is used to service the load; and the economic perspective is based on the evaluation of NPC and LCOE. The obtained results show that including a backup diesel generator in the proposed HRES strengthens the complementing abilities of supply and lowers the system's fuel costs, LCOE, and GHG emissions.

A hybrid system's lifespan and cost are significantly influenced by the choice of energy generation sources, component combinations, and energy dispatch strategy [9–11]. This choice involves a thorough technical and economic examination of the HRES configurations to satisfy a given site's energy requirements based on the availability of RERs [12,13]. It is crucial to correctly size the generating system and choose the combination of energy sources in accordance with the electricity demand and RERs available at a specific site location in order to increase the system's efficiency while lowering its cost; only then will the system be efficient and cost-effective [14,15].

HRES component sizing is a continuous-type optimisation problem. When there are a large variety of possible design points, the standard iterative approaches are less efficient and take an exceptionally long computational time [16]. Therefore, numerous studies have employed various meta-heuristic algorithms to solve these kinds of optimisation problems. These techniques mimic problem-solving procedures utilised by organisms, making them more adaptable and providing a better solution than deterministic methods when solving optimisation problems. However, a particular meta-heuristic optimisation method may produce encouraging results when addressing one type of optimisation issue, but it may produce poor results when tackling a different kind of optimisation problem [17]. Shara and Elmekkawy [18] carried out a study, applying particle swarm optimisation (PSO) algorithm, on the best design for a stand-alone HRES comprising PV/wind/battery/H2 tank/-fuel cell/DG system to deliver power to a remote location in Zaragoza, Spain. An examination of the sensitivity of various parameters to the proposed model. Hazem and Hazem [19] implemented PSO algorithm-based HRES optimisation to reduce energy costs in a remote area in Brittany, France. The total NPC was introduced as the fitness function in the particle swarm process, taking into account the minimal fitness values. The PSO performed better when compared with previous algorithms. It presented a faster and more accurate result while also lowering total costs. Ajewole et al. [20] also performed a comparative analysis of three meta-heuristic algorithms in calculating the cost of a HRES. Bonferroni– Holm approach was utilised to ascertain the statistical significance among the algorithms. Using GA, PSO, and ABC, the optimum sizes of solar, battery storage (BS), and DGs that could be hybridised to satisfy the energy demand of a remote settlement in Nigeria were identified. It was concluded that ABC developed the optimal design consisting of 427 units of solar PV panels, 19 units of battery, and a 163.2 kW-rated DG. With this, a total annualised cost of $167,284 and 0.2443 LCOE was obtained. These were the lowest when compared with PSO and GA. Gharibi et al. [21] discovered the Pareto front of the multi-objective optimisation of an on-grid DG-PV-fuel cell HRES using a multi-objective crow search algorithm (MOCSA) for a town in Kerman, Iran. To maximise power flow between the hybrid system and the grid, two more choice factors are introduced to the study: the selling coefficient and purchasing coefficient. However, a few studies in Nigeria have been published on grid-connected hybrid systems using meta-heuristic techniques. Also, the popularity of application software like HOMER for HRES analysis, particularly in Nigeria, is evident from observed literature [4,22–24]. HOMER is a user-friendly software application that employs iterative approaches to analyse every potential system configuration, choose the best one, and. Nevertheless, it gives few options for power management techniques; as a result, it is hard to assess how well energy systems operate when using sophisticated power management strategies. Furthermore, since these software applications are "black-box" models, users cannot alter the control algorithm to address a particular situation.

Therefore, this study primarily focuses on optimising an HRES linked to an unstable utility grid and supported by a DG to increase the system's reliability while taking full advantage of locally available RERs. The key contribution of this study can be summed up as follows:

- Mathematical modelling of solar/wind/biogas/battery/diesel/grid hybrid power system.
- Developing an appropriate operational strategy for the HRES connected to an unreliable grid to cost-effectively and continuously meet the load profile of the case study.

Table 1
Information on Maizube farm.

Information on Maizube farm	
Farm Name	Maizube Farms Nigeria Limited
Latitude and Longitude	9°25′35″N 6°22′42″E(9.433821°N 6.375634°E)
Elevation	191 m ASL
Distance from Minna	26 km
Area of farm site	500-hectares
Farm Products	Milk, Yoghurt, and fruit juice
Quantity of Milk processed daily	1000 litres
Types of non-grazing Cows on farm	Red Friesians and Holstein Friesian
Number of non-grazing Cows farm	126
Types of grazing Cows on farm	Sokoto Godali and white Fulani (Yankanaji)
Number of grazing Cows on farm	191

- Conducting a techno-economic analysis of the HRES utilising ABC, GA, and PSO algorithms to examine the possibility of harnessing locally accessible RERs to satisfy the energy requirements of a case study.
- Performing comparative analysis of the best result from the ABC/GA/PSO algorithm to the result obtained from HOMER Pro software.
- Comparing the cost and GHG emissions of the proposed HRES with that of the pre-existing energy system configuration of the case study.

This paper is divided into seven sections. Section 2 contains information on the case study and available energy resource data. Section 3 presents the mathematical modelling of various system components. Section 4 covers the problem formulation and proposed operational strategy. Section 5 briefly introduces the metaheuristic techniques employed in this study. Section 6 presents and discusses the obtained results. Section 7 is the conclusion.

2. Description of the case study site

The Maizube farm was chosen for this study because of its high potential for biomass and solar energy resources. The farm is located in Sabon Dagah (9°25′35″N 6°22′42″E), a rural village on the outskirts of Minna, Niger state, Nigeria. The farm is divided into several sections or units, including the Cowshed, Feed processing centre, Milking parlour, Milk processing unit, Orchard, and Administrative department. The farm is connected to an unreliable grid and has standby diesel generatorss for power outages. An overhead perspective of the farm centre is presented in Fig. 1. Table 1 also contains additional information about the case study farm.

2.1. Case study farm load profile

The farm operates on a daily routine. Activities start from 8 a.m. to 5 p.m. on weekdays; however, milk is pumped from lactating cows at 4.30 a.m. and 4.30 p.m. every day (including Sundays) for about an hour. The farm electrical load, maximum power rating, and average daily usage are presented in Table 2. The load demand data was gathered via questionnaires and semi-formal interviews with dairy farm workers and engineers. Most of the electric loads are small-scale industrial loads such as ac fans, pumps, compressors, and light bulbs. The farm has an average daily electrical energy usage of 982.86 kWh/day (average load demand 40.95 kW), a peak power of 83 kW, and a load factor of 0.49.

Throughout the year, the case study area experiences three distinct seasons: the dry season (February to April), the rainy season (May to November), and the harmattan season (December to January) brought on by the cold, dry Harmattan winds from the Sahara Desert. During the dry season, the community's energy consumption is higher because loads such as air conditioners, fans, and water pumps are utilised more often to mitigate the impacts of the heat [25]. On the other hand, the relatively colder harmattan seasons have the lowest energy consumption. Fig. 2 shows the daily load requirement for each season.

2.2. National grid supply

The studied farm is connected to the public electricity grid. However, the electricity supply, like most of the country, is highly erratic, with an average grid supply of 7 h per day and a 70.8% probability of an energy blackout [25]. Fig. 3 illustrates the farm's grid power supply during a typical week.

Table 2
Breakdown of the studied location's daily energy demand for different seasons of the year.

S/N	Load Type	Quantity	Power rating (kW)	Feb. to Apr. (Dry season)		May to Nov. (Rainy Season)		Dec.& Jan. (Harmattan Season)	
				hrs/day	kWh/day	hrs/day	kWh/day	hrs/day	kWh/day
A. Milking Parlour									
1	Milk pumps	13	5	2	130	2	130	2	130
2	Compressor	1	2.5	2	5	2	5	2	5
3	Water heater	1	4.5	1	4.5	1	4.5	1	4.5
4	Water pump	1	5	2	10	2	10	2	10
5	Fans	10	0.5	2	10	2	10	0	0
B. Milk Processing Unit									
1	Homogenizer	1	30	3	90	3	90	3	90
2	Pasteurizers	20	1.5	6	180	6	180	6	180
3	Separator	3	3	3	27	3	27	3	27
4	Water heater	2	4.5	3	27	3	27	2	18
5	Water pump	1	5	2	10	1	5	2	10
C. Milk Cooling Unit									
1	Compressor 1	1	12	22	264	20	240	20	240
2	Compressor 2	1	6	22	132	21	126	20	120
D. Cow Shed									
1	Fans	15	0.5	18	135	14	105	6	45
2	Halogen lamps	34	0.4	8	109	10	136	10	136
3	Water Pump	1	3	1.5	4.5	1	3	1	3
E. Feed Processing Unit									
1	Elevator	1	5	3	15	3	15	3	15
2	Grinder	2	5	3	30	3	30	3	30
3	Feed processing machine	1	10	3	30	2	20	2	20
F. Miscellaneous loads			8	8	64	7	56	6	48
	Total Daily Demand				**1277**		**1219.5**		**1131.5**

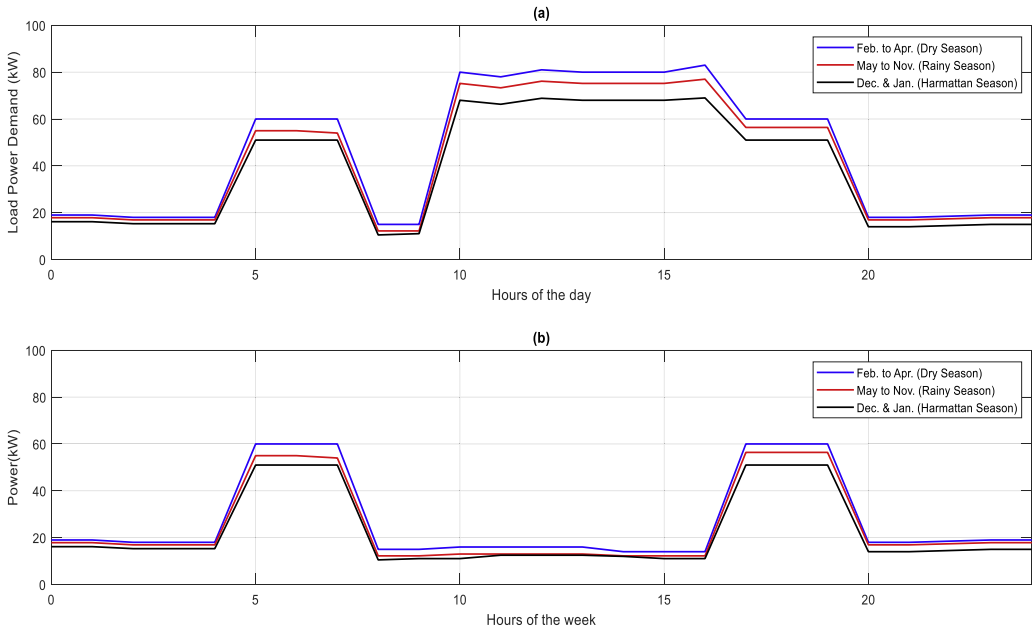

Fig. 2. Seasonal variation in the daily load profile of the case study location (a) load profile for weekdays and (b) load profile for weekends.

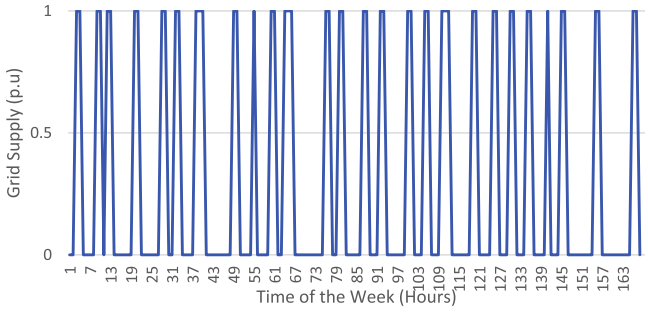

Fig. 3. Grid supply outages for the case study site in a typical week.

2.3. Solar resources

Nigeria is located within the tropical region and thus receives ample solar radiation all year [26]. Fig. 4 depicts the annual solar irradiance for the studied site obtained from the national aeronautics and space administration (NASA) solar energy and surface meteorology database [27].

Solar radiation is well distributed throughout the year at the site, with an average of 5.49 kWh/m^2/day and peaking at 6.26 kWh/m^2/day in March. The total solar energy potential of 2003.85 kWh/m^2/$year$ available to be converted to electricity. This indicates that the solar energy system is an appealing power source for the area. Fig. 5 represents the annual average temperature. The power production of solar PV is slightly negatively affected by its operating temperature [28].

2.4. Wind resources

The wind turbine's power production is highly dependent on wind speed, wind speed data is, therefore, an essential resource in the HRES study. Because wind speed statistics for the examined site were not accessible, wind speed information from NASA's renewable energy resource website [27] was utilised and is presented in Fig. 6. The monthly average wind speed ranges from 3.6 metres per second in December to 2.1 metres per second in October. The yearly average wind speed is 2.6 m/s, indicating a modest potential for wind power harvest.

2.5. Biogas resources

Cow dung and other organic matter can be used to produce biogas through anaerobic digestion and the biogas can then be used as fuel for generating heat and/or electricity. The farm also has over 300 cows on

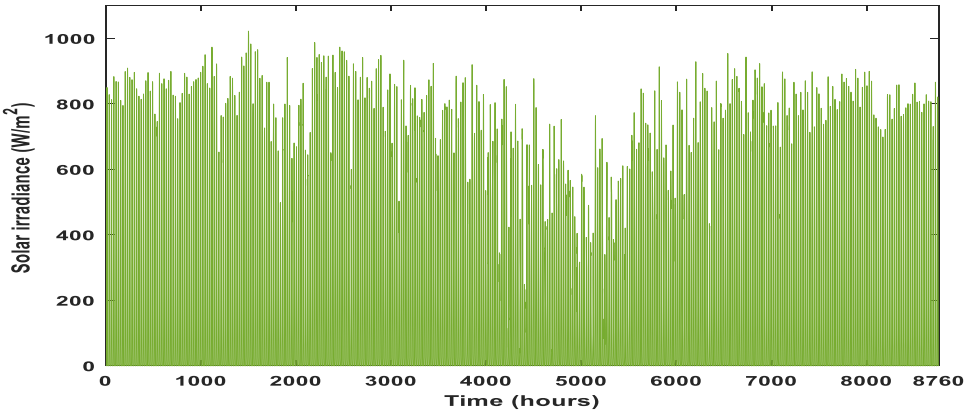

Fig. 4. Annual solar irradiance of the case study.

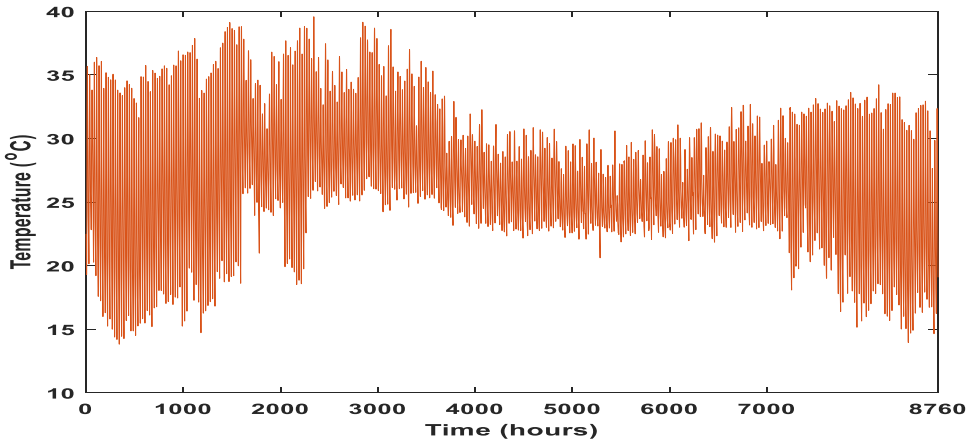

Fig. 5. Annual average temperature of case study location.

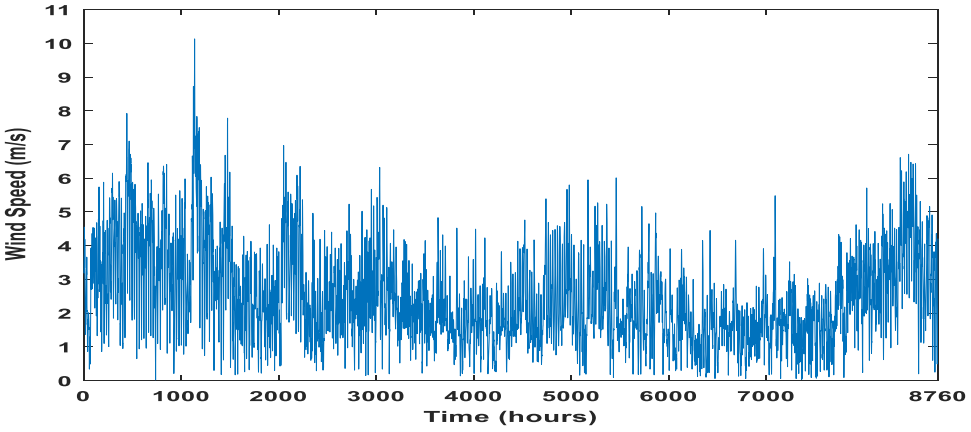

Fig. 6. Wind speed (m/s) at the studied location, 10 m above sea level.

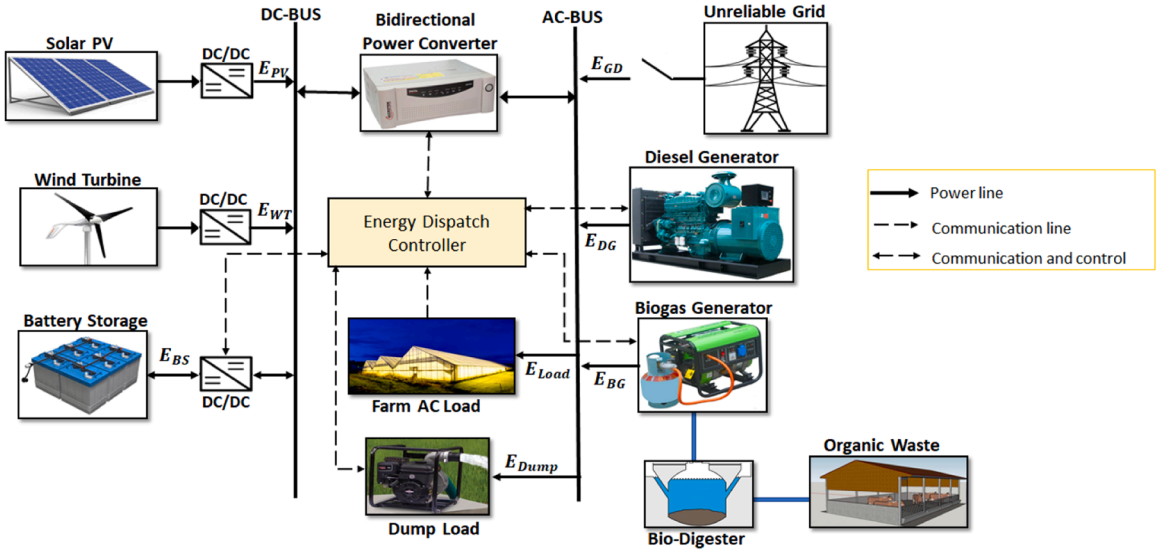

Fig. 7. The proposed hybrid energy system configuration.

site, as presented in Table 1. Each cow produces an average of 15 kg of dung a day. That is about 4500 kg of potential biogas resource daily at little or no cost.

This study proposes collecting the organic waste from the cow shed and utilising it as feedstock in a bio-digester to produce biogas. The main constituent of biogas produced is methane gas, which accounts for 60% to 70% of the total, with the rest being carbon dioxide (CO_2) and traces of hydrogen sulphide (H_2S), ammonia (NH_3), oxygen (O_2), nitrogen (N_2), and carbon monoxide (CO) [4].

3. Mathematical modelling of HRES components

The proposed grid-connected HRES is made up of various components such as solar photovoltaic (PV), wind turbine (WT), power converters (PC), utility grid (GD), battery storage (BS), biogas generator (BG) and diesel generator (DG) as illustrated in Fig. 7. DG is only utilized as a last resort and is only activated when other sources are insufficient to supply the load demand at a particular period. The power output of renewable sources is considered to be constant over the course of one hour. This section presents the mathematical modelling of the proposed in order to analyse its performance.

3.1. Solar PV model

Solar irradiance and ambient temperature at a given moment are two important input factors that might impact the power output of solar PV, and both were considered in this study. The mathematical model employed in this work to compute the power output of solar PV is based on the model described in [29,30].

$$\boldsymbol{P_{pv}(t)} = \boldsymbol{P_{pv\_r}} \times \boldsymbol{d_{rf}} \times \frac{\boldsymbol{G(t)}}{\boldsymbol{G_{STC}}}[1 + \boldsymbol{\psi_T}((\boldsymbol{T_{amb}} + (0.0256 \times \boldsymbol{G(t)})) - \boldsymbol{T_{STC}})] \tag{1}$$

Where, $P_{pv}(t)$ is the output power (W) of the solar PV at time t, P_{pv_r} represents the rated power (W) of the solar PV at standard test conditions (STC), d_{rf} is the derating factor of the solar panel, $G(t)$ is the hourly solar irradiance (W/m^2) incident at the surface of solar PV panel, G_{STC} *is the* solar irradiance at STC (1000 W/m^2), ψ_T is the temperature coefficient of the solar PV ($-3.7 \times 10^{-3}\ ^oC^{-1}$), T_{amb} symbolizes the ambient temperature (^oC), and T_{STC} indicates the PV cell's temperature at STC (25^oC).

3.2. Wind turbine model

Wind turbines are propelled by the wind's kinetic energy to produce electricity. Wind speed is the key determinant of a wind turbine's power production. Because wind speed varies with altitude, the wind speed at the recorded height must first be converted to the desired hub height using the wind profile power law equation expressed in Eq. (2) [31].

$$\boldsymbol{V_{hub}(t)} = \boldsymbol{V_{ref}(t)}\left(\frac{\boldsymbol{H_{hub}}}{\boldsymbol{H_{ref}}}\right)^{\alpha} \tag{2}$$

Where, $V_{hub}(t)$ is the wind speed (m/s) at the WT's hub height H_{hub} (m) and $V_{ref}(t)$ is the reference wind velocity (m/s) at the anemometer height H_{ref} (m), α denotes the friction coefficient (also called the Hellmann exponent). The value of α depends on factors such as wind velocity, temperature, terrain contour, and height above ground. The typical value of α is 1/7 for well-exposed locations with low surface roughness [6].

The hourly power generated by the WT ($P_{WT}(t)$) is determined using the power curve equation [32].

$$\boldsymbol{P_{WT}(t)} = \begin{cases} 0 & \boldsymbol{V_{hub} < V_{cut-in}\ or\ V_{hub} \geq V_{cut-out}} \\ \boldsymbol{P_{WT.R}}\left(\frac{\boldsymbol{V_{hub}^3}}{\boldsymbol{V_R^3 - V_{cut-in}^3}}\right) - \boldsymbol{P_{WT.R}}\left(\frac{\boldsymbol{V_{cut-in}^3}}{\boldsymbol{V_R^3 - V_{cut-in}^3}}\right) & \boldsymbol{V_{cut-in} \leq V_{hub} < V_R} \\ \boldsymbol{P_{WT.R}} & \boldsymbol{V_R \leq V_{hub}(t) < V_{cut-out}} \end{cases} \tag{3}$$

Where, P_{WT_R} (kW) is the WT's rated power, V_{hub} (m/s) signifies the wind velocity at WT's hub height, V_R(m/s) represents the rated wind speed of the WT, V_{cut-in} and $V_{cut-out}$ denotes the cut-in and cut-out wind speed of the WT, respectively.

3.3. Biogas generator model

The availability of cattle manure at the case study location (dairy farm) ensures the continuous supply of biogas resources that can produce heat or/and electricity for the case study location. Waste-to-energy has the potential to be both a long-term carbon-neutral and ecologically friendly energy source and a feasible alternative to conventional fuels [4]. A biodigester and a biogas engine make up a biogas generation system. The gas engine is linked to the gas pipeline and receives biogas from the biodigester's gas tank. Like a traditional diesel engine, the biogas engine uses an integrated generator to convert biogas into electricity. The digester tank is fed with organic materials, and the gas burner and gas generator are linked to the biogas pipe's outlet. The volume of biogas (m^3) the system can create in a day is a measure of its capability [33,34].

Energy can be released when the methane in the biogas is burned or oxidized with oxygen. Hence, the direct burning of biogas for heating or its use in gas engines to produce heat and power. About 25% of the energy is saved when converting biogas to electricity, and 55% is saved when burning it to provide heat [34].

Eq. (4) is used to determine the amount of electric energy (E_{BG}) measures in KWh that can be generated from the available organic waste [33].

$$\boldsymbol{E_{BG}} = \boldsymbol{P_{BG}} \times \boldsymbol{h_{BGG}^{yr}} \tag{4}$$

where P_{BG} (kW) and h_{BGG}^{yr} the BG's power rating and the annual operation hours of BG (hr/year), respectively. Eq. (5) determines the maximum BG power rating (P_{BG}^{max}) for the proposed system in kW.

$$\boldsymbol{P_{BG}^{max}} = \frac{\boldsymbol{M_{BM}} \times \boldsymbol{V_{BG}} \times 1000 \times \boldsymbol{CV_{BG}} \times \boldsymbol{\eta_{BGG}}}{860 \times \boldsymbol{h_{BGG}^{yr}}} \tag{5}$$

Where M_{BM} denotes the total amount of biomass (ton/yr) available for electricity production in a year, V_{BG} the specific biogas volume from the organic waste (m^3/ton). CV_{BG} represents the calorific value (kcal/m^3) of biogas, and η_{BGG} is the overall BGG conversion efficiency.

3.4. Diesel generator model

Diesel generators are compression ignition engines combined with an alternator. The generator converts chemical energy (diesel) to electrical energy. The fuel consumption of a DG is determined by the generator's size and the load under which it operates. Most generators operate at 80% to 100% of their rated power. Eq. (6) may be used to calculate the fuel usage (F_c) of a DG in litre/kWh [21].

$$\boldsymbol{F_c} = \boldsymbol{AP_o(t)} + \boldsymbol{BP_r} \tag{6}$$

Where P_o and P_r indicate DG's operational power output in kW at time t and DG power rating (in kW), respectively. A and B are the chosen DG's fuel curve gradient in $litre/kWh$, and the DG's fuel curve intercept coefficient in $litre/kWh$, respectively. For the selected generator, A and B have values of 0.246 and 0.0842, respectively [35].

3.5. Battery storage model

Batteries are used in HRES to store excess energy and discharge it when renewable energy is insufficient or unavailable. The battery bank's capacity is determined by the electrical load requirement and the number of days the BS is expected to supply power to the load when the RES output is insufficient to meet the energy demand (known as autonomy days D_a). Since the HRES consists of DG that can be dispatched in the worst-case scenario when no other power source is available, the $D_a$considered is one day. The required cumulative rating of the battery bank (R_{BS}) in ampere-hour (Ah) can be calculated as follows.

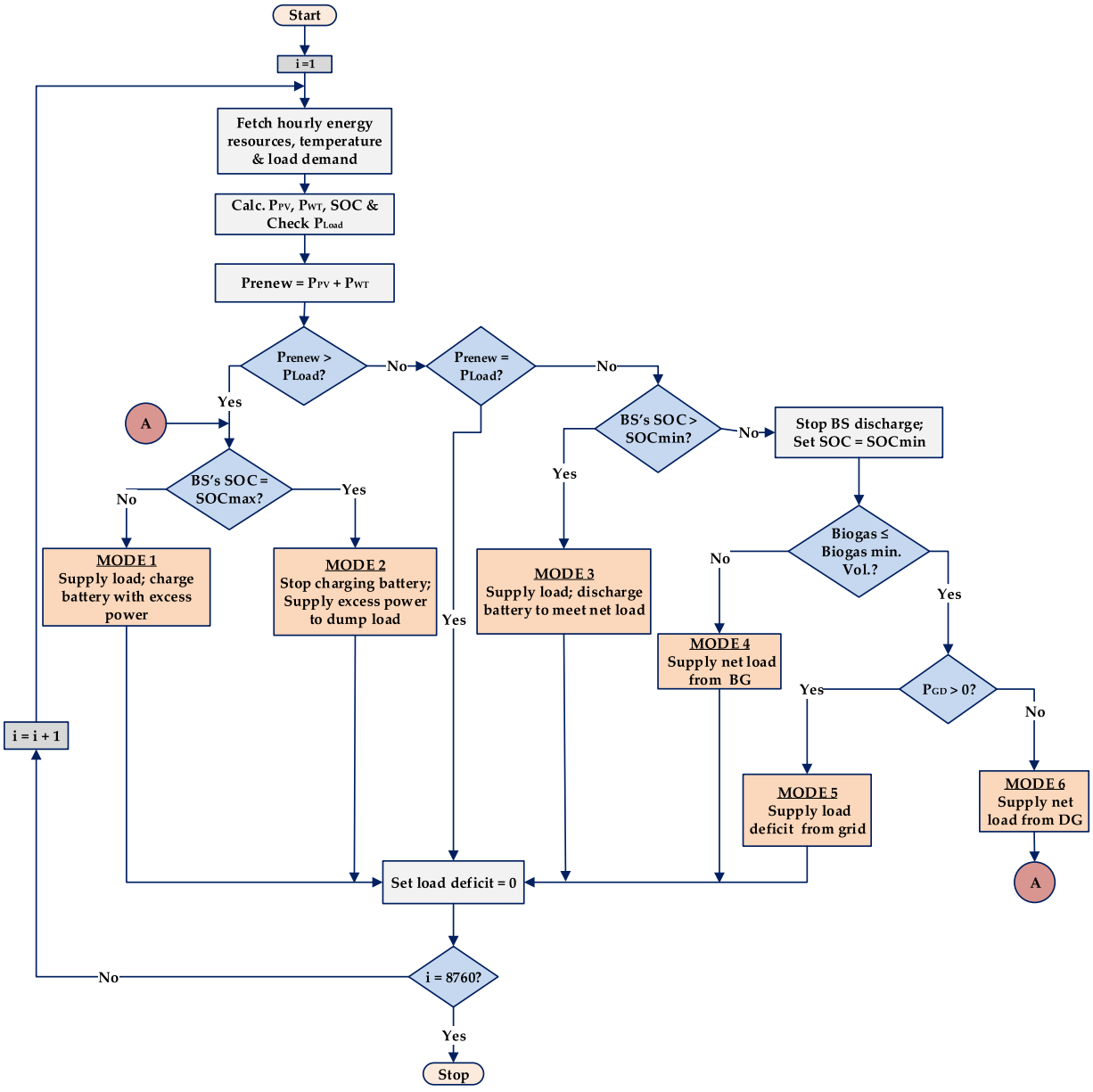

Fig. 8. Flow chart of the proposed operational strategy for system component size optimisation.

$$R_{BS} = \frac{P_{Load} \times h_{BS} \times D_a}{\eta_{BS} \times DoD_{max} \times V_{BS}} \times 1000 \quad (7)$$

Where P_{Load} is the load required (kW) to be met by the BS, h_{BS} denotes the number of hours per day the BS supplies power (hr/day), $D_a$signifies the autonomy days, η_{BS} represents the battery's round-trip efficiency, DoD_{max} is the battery's maximum depth of discharge, and V_{BS} is the battery bank's normal voltage.

The number of batteries required can be determined as follows:

$$N_{BS} = \frac{R_{BS}}{R_{1\_BS}} \quad (8)$$

Where R_{1_BAT} is the rated capacity of a single battery in ampere-hours (Ah).

To produce the required bus voltage, batteries are linked in series. (V_{bus}). The number of series-connected batteries (N_{BS}^{S}) can be calculated as follows:

$$N_{BS}^{S} = \frac{V_{bus}}{V_{1\_BS}} \quad (9)$$

Where V_{1_BS} is the nominal voltage rating of the battery unit.

The battery behaviour is mainly characterized by the state of charge (SOC) at an instance t, measured in percentage of the battery-rated capacity. SOC is the reciprocal of DOD (i.e. SOC = 1 − DOD) and can be determined using Eq. (10) as given by [36,37].

$$SOC(t) = SOC(t-1) + \frac{\sum N_i P_i(t) - P_{load}(t)}{V_{BAT} C_{BAT}} \quad (10)$$

Where i is the power generator indicator, N_i is the number of generator units i and P_i is the power output for generator unit i at time t. Where $i \in \{PV,\ WT, GD, DG,\ BG\}$

3.6. Power converter model

When both alternating current (AC) and direct current (DC) com-

ponents are in the system, DC/AC and AC/DC power converters are required. Solar PV, WT, and BS provide DC power, whereas the considered load requires an AC power supply. Also, AC power from DG, BG, and grid can be required to be converted to DC needed to charge the battery storage. The converter capacity (P_{PC}^{max}) is determined by the peak load demand (P_L^{max}).

$$P_{PC}^{max} = \frac{1.2\ P_L^{max}}{\eta_{PC}} \tag{11}$$

Where, η_{PC} is the converter efficiency.

4. Optimisation problem formulation

As earlier stated, this study aims to design a reliable and affordable HRES. The main deciding factors are the optimal capacity sizing of PV, WT, BS, DG and BG. This section contains information about the system's energy dispatch strategy, reliability, objective function, and system constraints. A brief overview of the algorithms used is also provided.

4.1. Proposed energy dispatch strategy

Getting all the HRES components to operate wholistically can be challenging. Therefore, in addition to component sizing, the energy management of the HRES must be optimal for a reliable and cost-effective system [38,39]. In this study, the diesel generator is given the least priority. It is only activated when the RESs and the BS cannot match the load requirement, and there is no power supply from the grid. Taking into account places with intermittent grid supply, the grid availability was considered stochastic, with a 30% chance of being available [40].

The algorithm monitors load demand and electrical energy available at each time step. The netload is the difference between the total power obtainable from RERs and the load demand $\left(P_{Net}(t) = \frac{P_{Load}(t)}{\eta_{pc}} - P_{PV}(t) - P_{WT}(t)\right)$. Fig. 8 depicts a simplified flowchart of the proposed dispatch strategy. The following modes are used to resolve the netload in order to cover all possible operating conditions and supply energy to the load at all times.

- *Mode 1 - Battery charging strategy*: if the total energy provided by renewable energy sources exceeds the load requirement at a given time interval ($P_{Net}(t) < 0$) and the SOC of the battery has not attained the predetermined maximum ($SOC(t) < SOC_{max}$), the battery storage is used to absorb the surplus power else, Mode 2 is activated.
- *Mode 2 – Energy dumping strategy*: There are no policies in place that support the exporting of energy to the national grid in Nigeria. As a result, when the sum of energy provided by RESs exceeds the load demand at a given moment, and the SOC of the battery bank is at maximum, then the surplus energy is supplied to the dump loads. Dump loads are typically deferrable loads like water pumps and heaters. This strategy aids in the prevent the battery bank from being damaged due to overcharging.
- *Mode 3 - Battery discharging strategy*: In a specific time interval, if the RESs are insufficient to meet the energy required by the load ($P_{Net}(t) > 0$) and the SOC is higher than the predetermined minimum level ($SOC(t) > SOC_{min}$) then, energy stored in the BS is dispatched to supply energy shortage.
- *Mode 4 - Biogas generator supply strategy*: When RESs and energy stored in battery banks are unable to fulfil the energy requirement of the load, then the BG is engaged to meet the netload.
- *Mode 5 – grid supply strategy*: When the load demand is higher than the total energy produced by Solar PV, WT, BS, and BG, then power is supplied from the national grid, if the grid power supply is available ($P_{GD}(t) > 0$), else Mode 6 is activated.
- *Mode 6 – Diesel generator supply strategy*: Finally, if the energy generated by the combined RESs and the energy stored in the battery is insufficient to meet demand and there is no grid power supply, then the DG is dispatched to meet the energy shortfall.

4.2. Objective function

The objective function of this Optimisation problem is the minimisation of the LCOE to determine the optimal size of the HRES component that will reliably meet the farm's energy requirement at the lowest cost. LCOE is the average cost per kWh of the energy produced by the system over its determined lifespan. The LCOE value allows the comparison of different energy system configurations on a similar scale. LCOE can be expressed as a ratio of the annualised system cost (ASC) ($\$ yr) to the average annual energy generated by the system E_{ann} (kWh/yr) . The objective function is expressed in Eq. (12).

$$\textbf{\textit{Minimise}}\ :\ \textbf{\textit{LCOE}}(\$/\textbf{\textit{kWh}}) = \frac{\left(\sum N_j C_j\right) + P_{Grd} C_{Grd}}{E_{ann}} \tag{12}$$

Where the number of component j (N_J) is the decision variable considered in this study and includes the number of Solar PV (N_{PV}), number of WT (N_{WT}), number of BS (N_{BS}), number of BG (N_{BGG}), number of DG (N_{DG}).

$$C_j = C_j^{ACAP} + C_j^{AO\&M} + C_j^{AREP} - C_j^{ASLV} \tag{13}$$

C_j is the annualised cost of a unit of component j, P_{Grd} is the annual amount of energy bought from the national grid (kWh/yr) and C_{GD} is the unit cost of electricity from the grid in $/kWh.The overall cost of each component unit (C_j) includes the annualised capital cost (C_j^{ACAP}), annualised operational and maintenance costs ($C_j^{AO\&M}$), annualised replacement cost (C_j^{AREP}), and salvage value (C_j^{ASLV}) which is subtracted from the total system cost as expressed in Eq. (13).

4.2.1. Annualised capital cost

The annualised capital cost is the component's principal cost, which includes the procurement and installation cost of the components. The annualised capital cost of each system component can be computed using the capacity recovery factor (CRF), which is a coefficient used to compute the equivalent annual cost as shown in Eq. (14):

$$C_j^{ACAP} = C_j^{CAP} \times CRF \tag{14}$$

Where $C_j^{CAP}$is the upfront capital cost of component j.

Given the component j's lifespan in years (L_j) and interest rate r, the CRF can be determined as thus [41]:

$$CRF = \frac{r(1+r)^{L_j}}{(1+r)^{L_j} - 1} \tag{15}$$

4.2.2. Operation and maintenance cost

The cumulative cost of O&M a unit of component j ($C_j^{AO\&M}$) includes labour costs as well as the cost of consumables (fuel, engine oil, spare parts, etc.) required to keep the component operational. The annualised value can be expressed as in Eq. (16).

$$C_j^{AO\&M} = H_j C_j^{O\&M/h} \times CRF \tag{16}$$

Where H_j is the number of operational hours of component j throughout its lifespan and $C_j^{O\&M/h}$ is the hourly operational and maintenance (O&M) cost of component j. For DG, the fuel cost is included in the O&M cost and is equal to the average amount of diesel consumed by the generator in a year (in litres) multiplied by the cost of one litre of diesel. The total fuel cost (C_{DG}^f) can be calculated as:

$$C_{DG}^f = E_{DG} C_f F(t) \times CRF \tag{17}$$

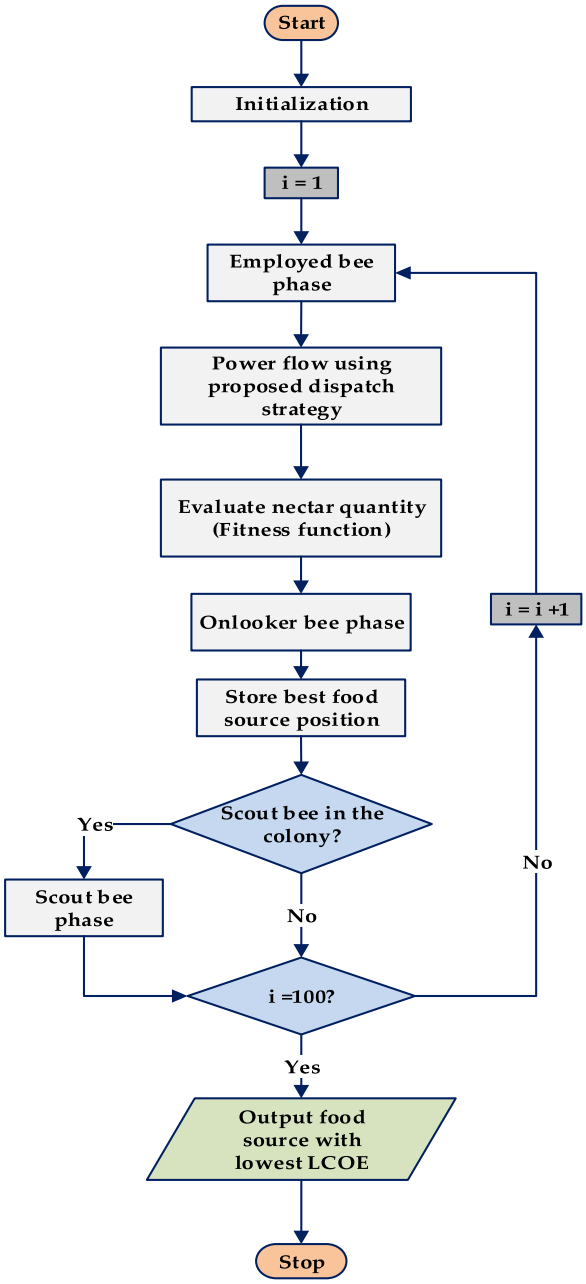

Fig. 9. Simplified process of the optimal sizing algorithm using ABC technique.

Where E_{DG} is the total energy produced by DG. C_f is the cost of a litre of diesel ($/litres) and $F(t)$ is the fuel consumption rate of the DG in litres/kWh.

4.2.3. Replacement cost

If the project's lifespan exceeds the component lifespan, replacements are necessary. The replacement cost of any system component is the cost of replacing the component at the end of its lifespan. The annualised replacement cost, C_j^{AREP}, throughout the project's duration can be expressed as: which took place over a project's duration might be expressed as

$$\boldsymbol{C_j^{AREP}} = \boldsymbol{C_j^{REP}} \times \boldsymbol{CRF} \times \frac{1}{(1+\boldsymbol{r})^{L_j}} \tag{18}$$

Where C_j^{REP} is the cost of replacing component j. In the case of DC and BG, lifespan is the total number of operating hours. The life span in years

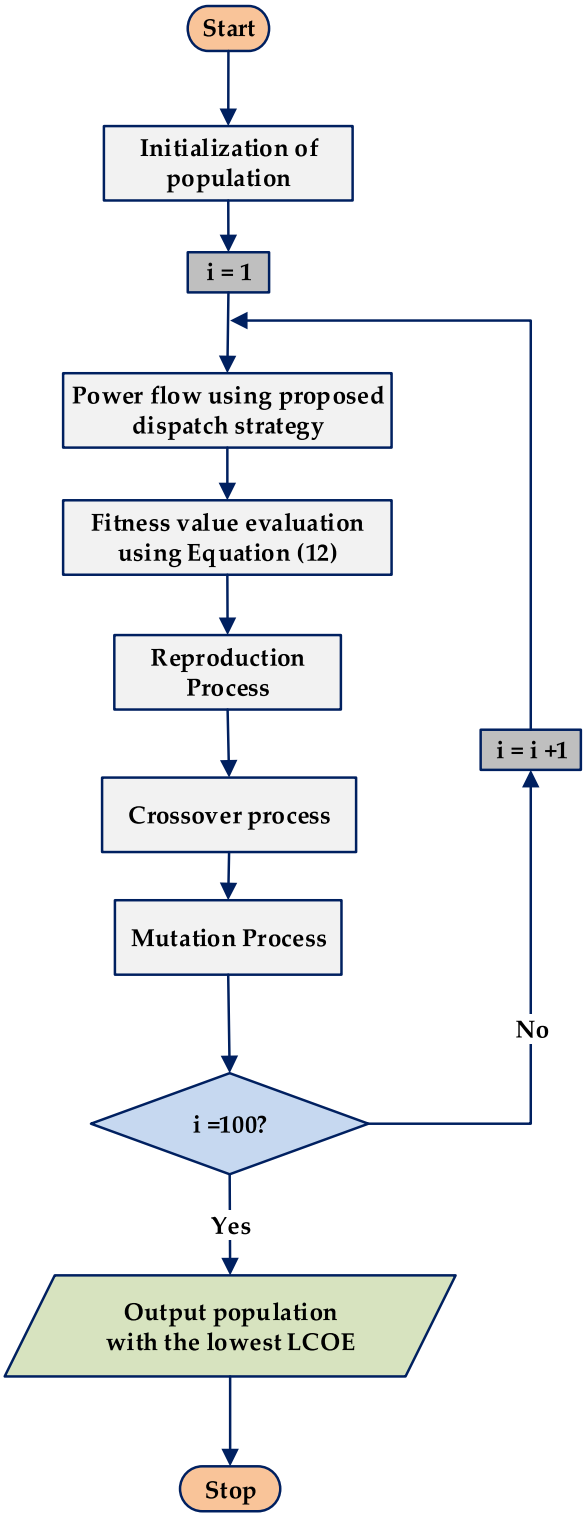

Fig. 10. Simplified process of the optimal sizing algorithm using GA technique.

of a diesel/BG (L_{Gen}) can be computed as expressed in Eq. (19).

$$\boldsymbol{L_{Gen}} = \frac{\boldsymbol{H_{Gen}}}{\boldsymbol{h_{Gen/y}}} \tag{19}$$

Where H_{Gen} and $h_{Gen/y}$ are the diesel/BG's lifespan (hours) and the number of hours of operation in a year, respectively.

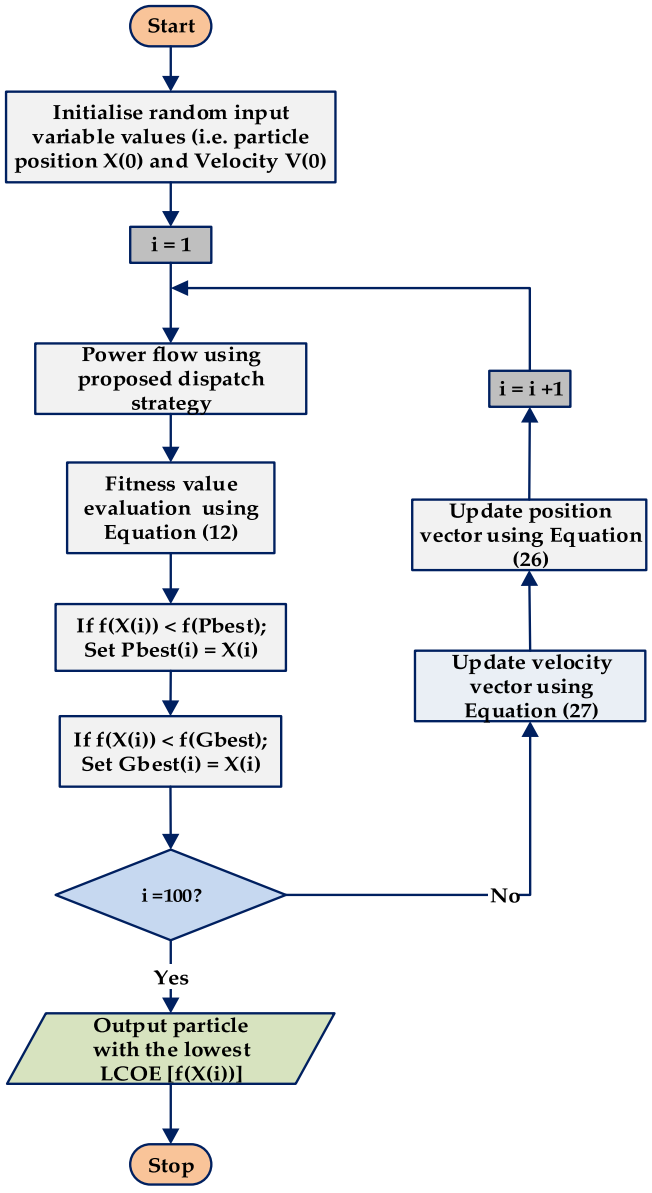

Fig. 12. Simplified process of the optimal sizing algorithm using PSO technique.

4.2.4. Salvage value

The salvage value is the component's projected resale value at the end of the project's lifespan. The annualised net present salvage value of a component j (C_j^{ASLV}) can be determined as a fraction of the replacement cost as shown in Eq. (20).

$$C_j^{ASLV} = C_j^{REP}\frac{L_j^{Rem}}{L_j} \times \frac{1}{(1+r)^{L_j}}\, CRF \tag{20}$$

Where, C_j^{REP} is the replacement cost of the component j, L_j^{Rem} is the remainder of the component's lifespan (in years) of component j at the end of the HRES lifespan and L_j is the total lifespan (in years) of component j.

4.2.5. Grid supply cost

Aside from system component-related costs, the cost of power exchange between the HRES and the utility grid is another key economic component to consider in grid-connected systems. Due to Nigerian legislative limits, the proposed HRES is designed to only purchase electricity from the grid. Grid purchase cost is the average annual cost of energy drawn from the national grid over the lifetime of the HRES. The total amount of electricity acquired from the grid, E_{GD} is expressed in Eq. (21).

$$E_{GD} = \sum_{0}^{8760} P_{GD}(t) \tag{21}$$

Therefore, the total price of energy bought from the grid in a year (C_{GD}) can be expressed as in Eq. (22).

$$C_{GD} = E_{GD}C_{GD}^{/kWh} \tag{22}$$

Where, $C_{GD}^{/kWh}$ is the unit cost of electricity ($/kWh) purchased from the grid.

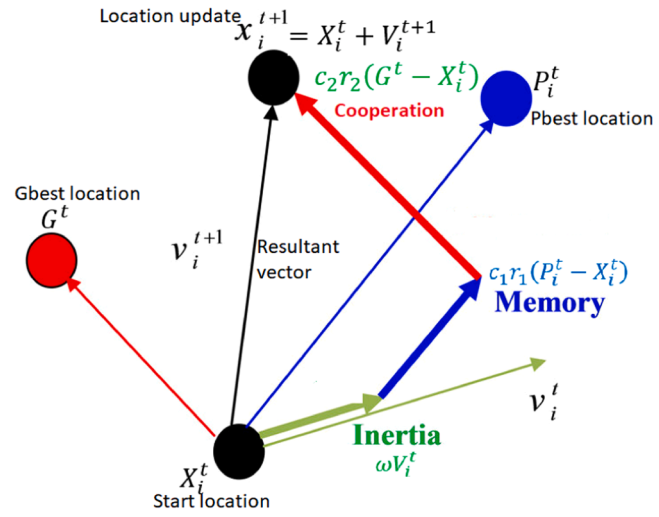

Fig. 11. Dynamic of particles in PSO.

Table 3
Optimisation control parameters.

ABC algorithm		PSO algorithm		GA algorithm	
Parameter	Value	Parameter	Value	Parameter	Value
Dimension of the problem (D)	5	Dimension of the problem (D)	5	Dimension of the problem (D)	5
Employed bees	50	Dimension of the problem (D)	5	Population size (N)	50
onlooker bees	50	Population size (N)	50	Distribution index for crossover	20
Colony size (NP)	20	Minimum weight (Wmin)	0.2	Distribution index for mutation	20
Food number	50	Maximum weight (Wmax):	0.9	Crossover probability	0.8
Limit (No of food × dim)	250	Maximum iterations (Itmax)	100	Mutation probability	0.2
Maximum iterations (It_{max})	100	Maximum iterations (It_{max})	100	Maximum iterations (It_{max})	100

4.3. System constraints

This system's optimisation is subjected to practical or/and technical constraints that must be met in order to generate viable solutions. The first constraint expressed in Eq. (23), is the energy balance between the

Table 4
Economics and technical specification of various components of the proposed system.

S/N	Component	Parameter	Value	Unit
1.	Grid	Grid capital cost	0	$
		Import energy tariff	0.07	$/kWh
		Export energy tariff	0	$/kWh
2.	Solar PV	Capital cost	1200	$/kW
		Replacement cost	1000	$/kW
		Operation and Maintenance cost	5	$/yr
		Lifetime	25	years
		Efficiency	20	%
		De-rating factor	88	%
		Temperature coefficient	−038	%/°C
3.	Wind turbine	Power output type	AC	
		Initial cost per unit	5000	$/kW
		Replacement cost	5500	$/kW
		Operation and Maintenance cost	50	$/yr
		Hub height	24	m
		Lifetime	20	years
4.	Battery Storage	Type	Lead-Acid	
		Capacity	1	kWh
		Initial cost per unit	300	$
		Replacement cost	250	$
		Operation and Maintenance cost	5	$/yr
		Maximum Depth of Discharge	20	%
		Throughput	800	kWh/yr
5.	Converter	Capital cost	300	$/kW
		Replacement cost	250	$/kW
		Operation and Maintenance cost	5	$/yr
		Lifetime	15	year
		Inverter efficiency	95	%
		Rectifier efficiency	95	%
6.	Biogas Generator	Rated capacity	5	kW
		Calorific value of cow dung	860.4	Cal/kg
		Conversion efficiency	25	%
		Initial cost	600	$/kW
		Replacement cost	600	$/kW
		O&M cost	0.1	$/hr
		Operation life	15,000	hour
7.	Diesel Generator	Initial cost per unit	195	$/kW
		Replacement cost	190	$/kW
		Operation and Maintenance cost	0.03	$/hr
		Lifetime	15,000	hours
		Conversion efficiency	30	%
		Diesel price	2	$/L
		Fuel curve slope	0.236	L/hr/kW
8.	Control parameters	Project lifespan	25	year
		Simulation time step	1	hour
		Annual capacity shortage	0	%
		Expected Inflation rate	12	%
		Interest rate	10	%
		Dispatch strategy	Cycle Charging (CC)	

power sources and the farm's load demand at all times.

$$\sum N_j P_j(t) \geq P_{load}(t) \tag{23}$$

Where $P_j(t)$ is the power output of a unit component j

The lower and upper constraints of the variables are presented in Eq. (24).

$$\textbf{\textit{Decision variables}} = \begin{cases} 1 \leq \boldsymbol{N_{PV}} \leq 2000 \\ 1 \leq \boldsymbol{N_{WT}} \leq 500 \\ 1 \leq \boldsymbol{N_{BS}} \leq 2000 \\ 1 \leq \boldsymbol{N_{BGG}} \leq 100 \\ 1 \leq \boldsymbol{N_{DG}} \leq 300 \end{cases} \tag{24}$$

The third constraint is the maximum and minimum charge level at which batteries may be charged or drained without compromising the longevity of the battery life cycle. This boundary is expressed in the following equation.

$$\boldsymbol{SOC_{min}} \leq \boldsymbol{SOC}(t) \leq \boldsymbol{SOC_{max}} \tag{25}$$

5. Optimisation techniques

In this study, ABC, GA and PSO optimisation techniques were adopted for the HRES sizing. The author directly picked optimisation approaches with the best performance and shortest operation time.

5.1. Artificial bee colony (ABC) algorithm

ABC is inspired by honey bee intelligence and can be used to solve various kinds of optimisation problems. This method imitates the co-ordinated social structure of the honeybee colonies. There are three main categories of honeybees in a colony; employed bees, onlooker bees, and scout bees [6]. The bees' search process can be summarised as follows and shown in Fig. 9:

1 At first, the employed bees will randomly choose a series of food source locations. The quantity of nectar the location produce will be evaluated, and they can store where food sources in their memory.

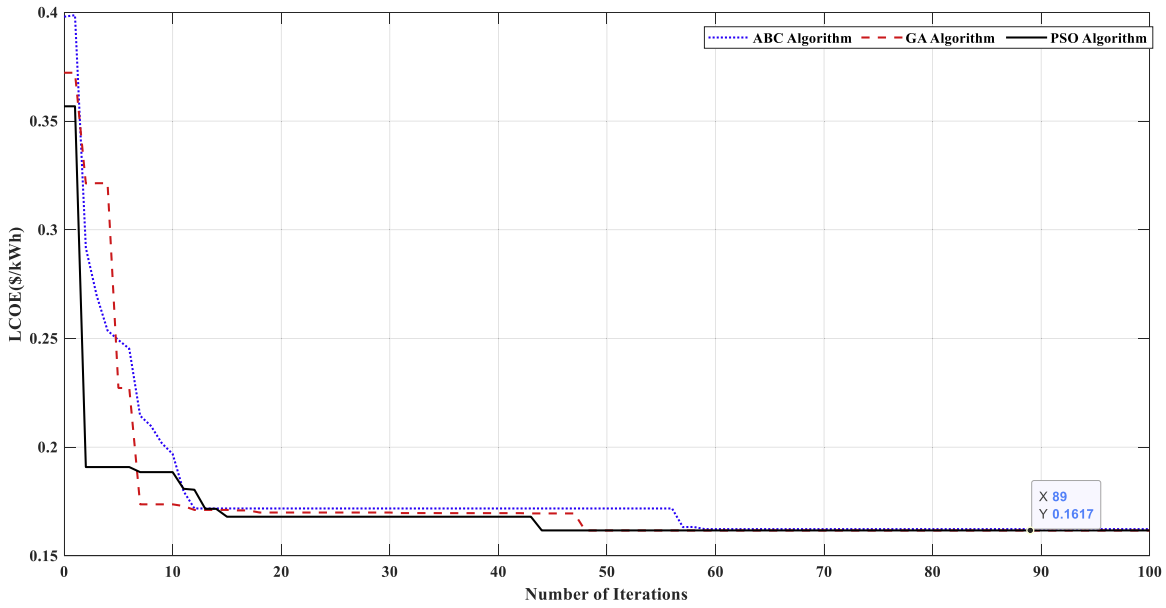

Fig. 13. Comparison of the convergence rate of ABC, GA, and PSO algorithm.

Table 5
Optimum system configurations for various techniques.

Proposed capacity								Economics	
Technology Algorithm	PV (kW)	WT (kW)	BS (kWh)	PC (kW)	BG (kW)	DG (kW)	Grid (kW)	NPC ($)	LCOE ($/kWh)
PSO	116	2	569	105	8	61	999.9	2.05M	0.162
GA	122	2	635	105	8	73	999.9	2.06M	0.163
ABC	135	3	643	105	10	88	999.9	2.11M	0.166
HOMER	119	2	574	100	10	64	999.9	2.08M	0.165

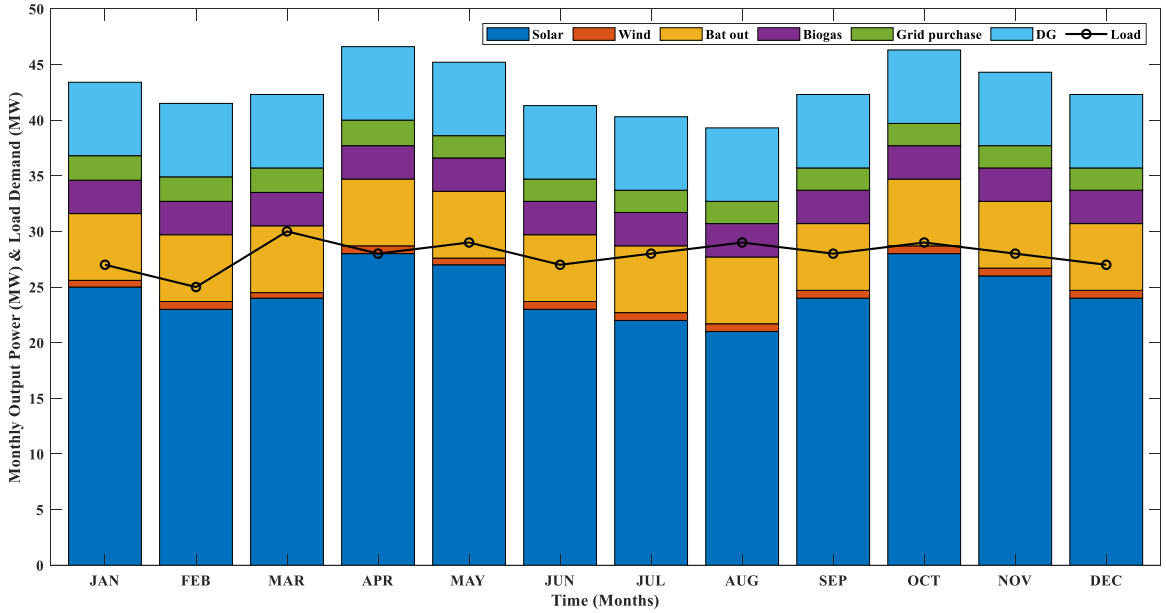

Fig. 14. Monthly energy production of various system units and load demand.

2 Afterwards, the employed bees return to the bee hive with specialised dances to communicate with the other bees about these food sources.
3 Based on the information provided by the employed bees, the onlooker bees go on to investigate the food sources.
4 Finally, after the food sources are abandoned, the employed bees become scout bees and randomly search the area to find new food sources.

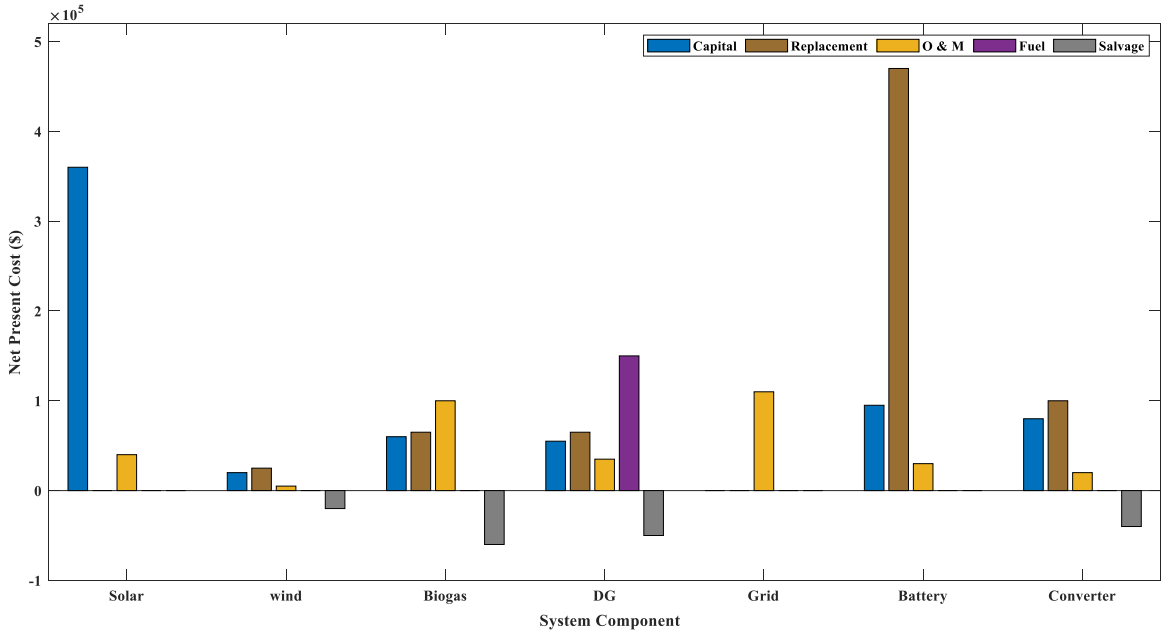

Fig. 15. Breakdown of the net present cost of various system components.

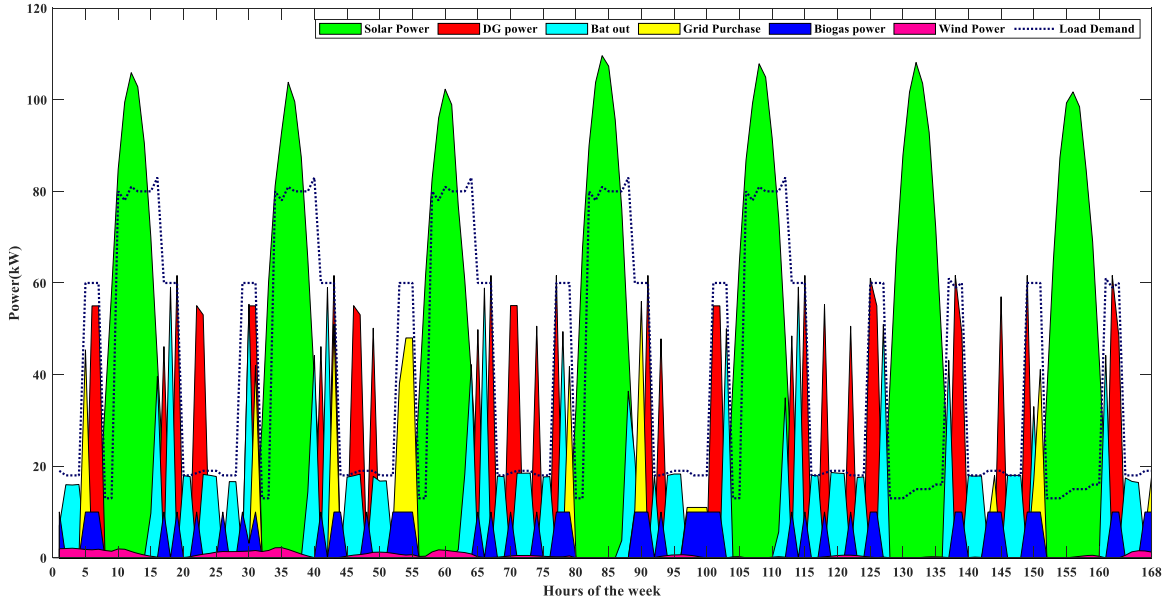

Fig. 16. Power contribution by various system components to meet the load demand for the fourth week in March.

5.2. Genetic algorithm (GA) algorithm

John Holland proposed the Genetic Algorithm (GA) in 1960–1970 [42]. It is a search algorithm modelled around the idea of evolution by natural selection. Typically, a population of randomly created individuals serves as the starting point for evolution. A *generation* is a term used to describe the population during each iteration of the operation. Fitness is assessed for each generation and population individually [43]. The fitness value represents the value of the objective function of the optimisation problem. The fittest members of the existing population are randomly selected, and their genomes are modified, recombined, or otherwise randomly altered to create a new generation. The algorithm then employs probable solutions from the following generation in its subsequent iteration. Usually, the process ends when the population has reached a desirable fitness level or the maximum number of generations have been generated [44]. An array of bits provides a standard representation of each proposed solution. A simplified flow chart of the GA process is presented in Fig. 10.

1 *Selection*: In this process, solutions with a high fitness value from each previous generation are chosen and used to form a new population. The fitness value of the function, which is the optimal function value, is used in the selection.
2 *Crossover*: In this procedure, the population with the highest fitness value is chosen from each subsequent generation. The crossover operation is performed by altering the bits of each population solution. This results in a new population with the highest fitness value, which can lead to improved solutions.
3 *Mutation*: is an operation that is used to distinguish the new generation from previous generations by modifying the bits of the current

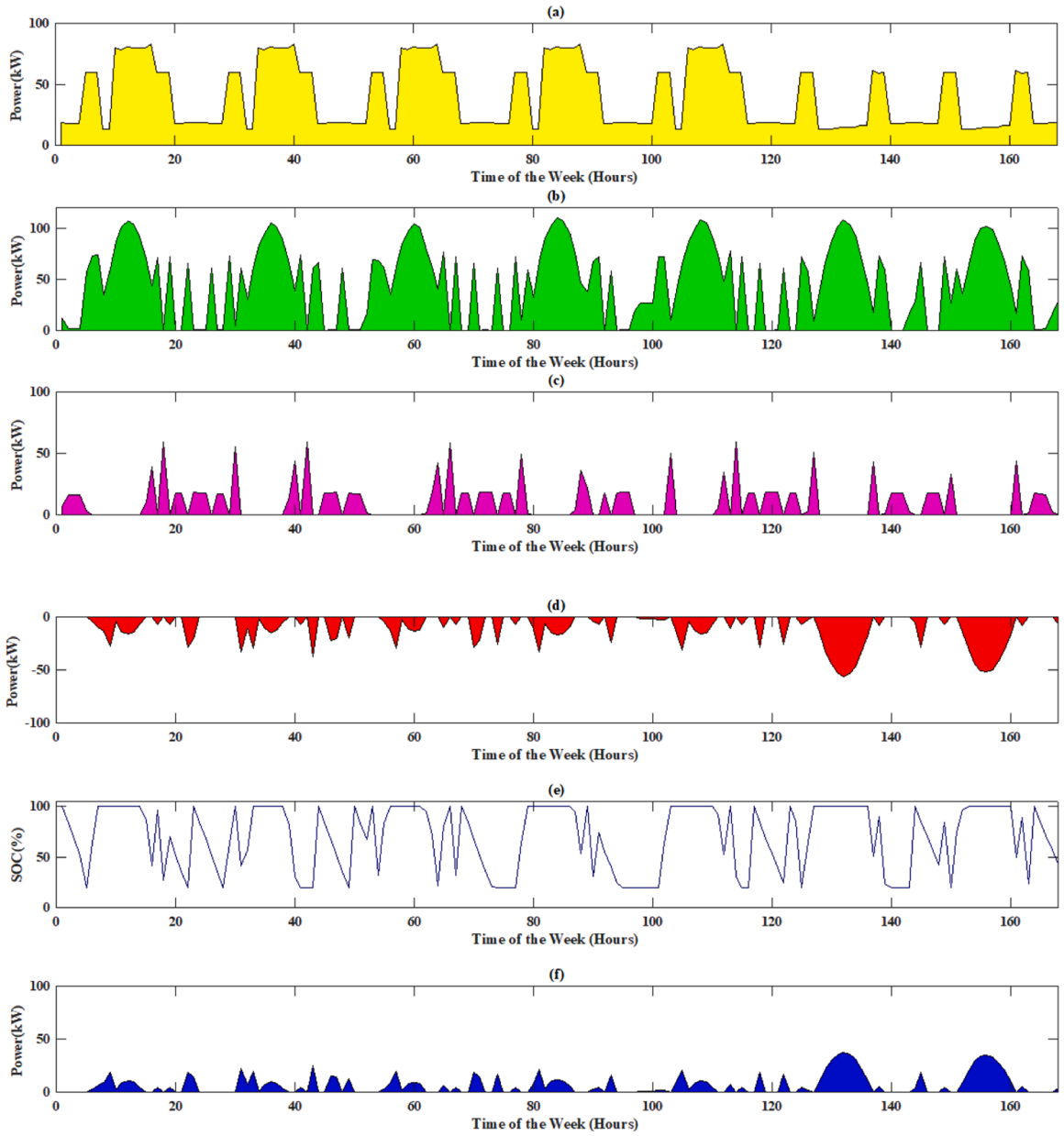

Fig. 17. Weekly comparison of power contribution by various components of the HRES (a) load weekly demand profile (b) combined power output from power generators (c) power output from the battery (d) power input to the battery (e) battery SOC (f) dump load.

generation if they are the same as the previous generation's population.

5.3. Particle swarm optimisation (PSO)

PSO is a meta-heuristic optimisation approach developed in 1995 by James Kennedy (Social-Psychologist), and Russell Eberhart (Electrical Engineer) is modelled after the social navigation of swarm organisms like a flock of birds or a school of fish First, a random number of particles or a population is formed using random location vectors and velocity vectors. The fitness value of each particle in the initial population is computed to evaluate its present location, which is then compared to its prior best experience (value). The personal best fitness values are compared to determine the global best value [45]. A simplified flow chart of the PSO algorithm is shown in Fig. 12.

If a particle's current position fitness value is better (i.e. greater for maximisation problems and lower for minimisation problems) than the best prior value attained, the particle's value is updated with the new value; otherwise, it is kept unchanged. In addition, the particle's velocity is changed based on the global best particle (Gbest) and its personal best experience (Pbest) [45,46].In each iteration, particles tend to gravitate toward the best global particle. The best global particle is then updated. Fig. 11 is a vector diagram exhibiting particle dynamics in PSO.

Each particle modifies its position by using the following information

- Their present positions (X_i^t).
- Their present velocities, (V_i^t).
- The difference between their present position and their personal best value, often known as Pbest (P_i^t).
- The difference between their present position and their global best value, often known as Pbest (G^t).

The following equations can modify the velocity and position of each particle.

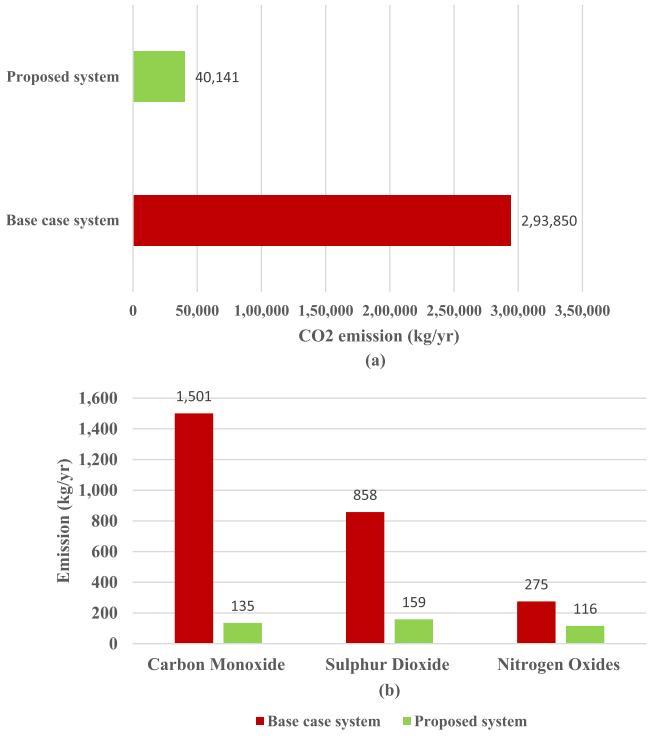

Fig. 18. GHG emission comparison: (a): CO2 emissions (b): Other gases.

$$X_i^{t+1} = X_i^t + V_i^{t+1} \tag{26}$$

$$V_i^{t+1} = \omega V_i^t + c_1 r_1 \left(P_i^t - X_i^t\right) + c_2 r_2 \left(G^t - X_i^t\right) \tag{27}$$

Where: X_i^{t+1} is the particle's position in the subsequent iteration, V_i^{t+1} is the velocity for the next iteration, ω is the inertia weight or coefficient, c_1 and c_2 are the respective acceleration factors (weights) for the cognitive and social factors, r_1 and r_2 are two uniform random numbers between 0 and 1 and are used to preserve the population's diversity [45].

6. Result and discussion

The optimal sizing of the proposed HRES using ABC, GA and PSO algorithms was carried out in a MATLAB 2020a environment on a personal computer fitted with an Intel Core i3–7100 Processor and 8GB RAM. The results of these metaheuristic techniques were then compared with those obtained from HOMER Pro software. The simulation is done on a year's worth of data with an hourly time step to meet energy demand. Table 3 presents the control parameter for the three metaheuristic techniques and Table 4 shows the technical data of various system components selected in this study (Fig. 12).

For the sake of comparison of findings, the highest and lowest number of solar PV panels, wind turbines, batteries, biogas generators, and diesel generators have been regarded as identical for all the algorithms. The size of the inverter is not a factor in the decision variable. Using Eq. (11), the inverter's rating is determined to be 105 kW based on the peak load demand. The optimal size of the system's component is determined based on the LCOE. Fig. 13 shows the convergence rates for PSO, GA, and ABC. It shows that PSO and GA converge to almost the same global minimum LCOE values. However, PSO performs better than

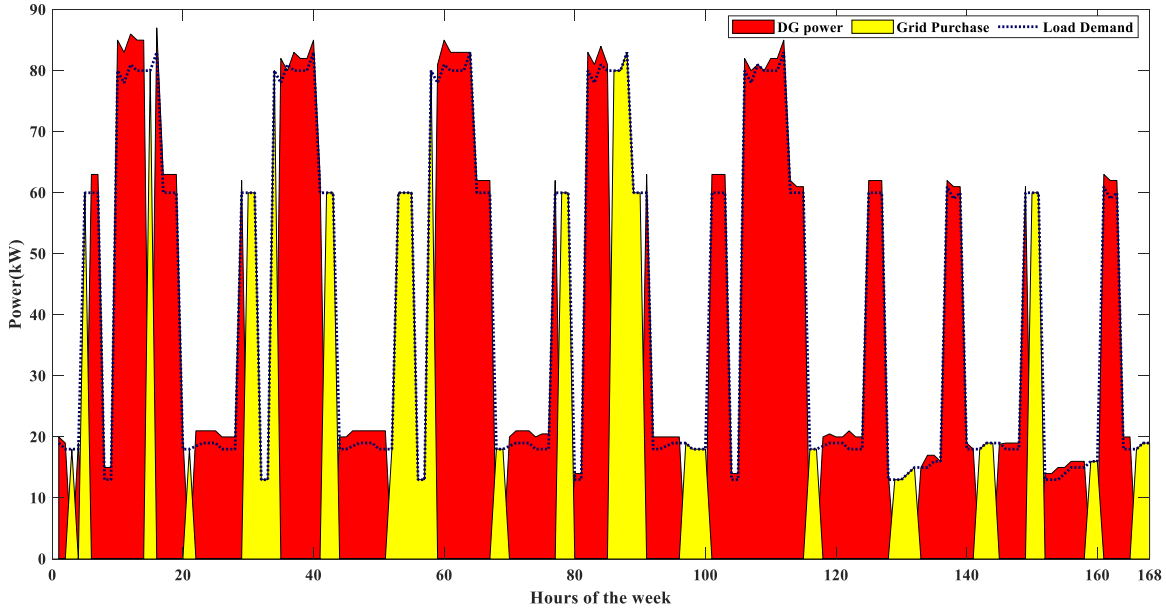

Fig. 19. The power contribution by base case system (national grid and backup DG) to meet the load demand for the last week in March.

Table 6
System configurations and cost comparison of the base and proposed power system.

Capacity									Economics			
Technology System	PV (kW)	WT (kW)	BS (kW)	PC (kW)	BG (kW)	GD (kW)	DG (kW)	Diesel usage (L/yr)	Initial cost ($)	ASC ($)	NPC ($)	Payback Period (yr)
Base System	–	–	–	–	–	999	250	84,351	31.5k	229.8k	9.56M	5.6
Proposed System	116	2	569	105	8	999	61	7.592	825.7k	82.3k	2.05M	

GA in terms of convergence time. Therefore, Therefore, the PSO algorithm's outputs are selected as the ideal combination for the case study and are compared with the result obtained from HOMER Pro for validation.

Table 5 shows the optimal component sizes obtained from PSO, GA, ABC, and HOMER to meet the total load demand of the studied location. The PSO algorithm proposes an HRES comprising 116 kW solar PV, 2 kW wind turbine, 569 kWh batteries, 8 kW biogas generator, and 61 kW diesel generator, which results in a system with an NPC of 2.05 million dollars and an LCOE of 0.162$/kWh.

The performance of the PSO algorithm is satisfactory in terms of result and convergence time when compared with HOMER Pro. Although HOMER pro converges a few minutes faster than the PSO algorithm, PSO slightly outperforms HOMER Pro in terms of optimal results.

Fig. 14 depicts the monthly energy contribution of various system units in meeting the load demand. The biggest portion of the energy generated comes from solar PV, accounting for about 64% of the annual energy production. In contrast, the lowest fraction comes from wind turbines, contributing less than 2%. This power production is consistent with the available RERs available at the case study location. The overall renewable fraction of the proposed system is 67.2%. Biogas contributes a significant 11% of the generation, demonstrating biogas's potential for generating reliable energy in an area with an abundance of organic waste.

Fig. 15 shows the net present cost of various system components. The studied location is already connected to the national grid; thus, the only cost constituent for the grid is the operating cost (cost of energy purchased from the grid). The battery storage needs to be replaced every five years. Therefore, it will be replaced four times in the project's 25 years, hence the high replacement cost. System components, wind turbines, BGs, DG, and converters that have not reached the end of their life span at the end of the project life can be sold at a salvage cost subtracted from the total system cost.

The power contribution by various components of the system to meet the load requirement for the fourth week in March, when the load demand is highest, is presented in Fig. 16. As described in the operational strategy, the DG is activated when power from renewable sources and batteries are insufficient to meet load demand, and there is no power supply from the national grid. In that week in March, the chart shows that solar, wind, and biogas power output is lower than load demand for a few hours (000–005); hence the battery is discharged to meet the energy deficit. At 005 h, the power supply from the grid is restored just in time for cow milking. However, the supply lasted only about one hour; hence, the DG is activated to supply the energy needed during cow milking. Between the hours of 008 and 014, owing to the increased availability of the solar resource, the power output from the solar PV in combination with the WT exceeds what is needed to meet the energy demand for milk processing. Thus, there is no need to run the DG and excess energy stored in the battery bank when energy output from RESs is low.

Fig. 17 shows the load demand profile for the entire week, combined power output from power generators, power output from the battery to meet renewable energy generation shortfall, and power input to the battery to absorb excess energy during surplus renewable power production. Hence, the battery's SOC varies throughout the week between the defined maximum of 100% and a minimum of 20%. It is observable from Fig. 17 that the SOC remains within the predetermined limit. It can be noted that there is a significant amount of excess energy from solar PV to be stored in the battery bank during the weekends due to little or no activities on the farm. Since there is currently no facility or policy in Nigeria that permits the sale of surplus energy to the grid, when the SOC of the battery reaches 100%, the surplus energy, if any, is used to power deferred load like pumping water to a reservoir or for irrigation.

6.1. Economic comparison

A comparative analysis of the proposed system and existing system (grid backed up with 250kVA DG) is carried out. With the base case as the control, it is computed that the initial cost of the proposed optimal system is 25 times that of the base system. However, with relatively low O&M cost, the NPC of the proposed optimal system is 78.5% less the that of the base system.

Making the proposed system cost-effective in the long run. The Payback Period was computed to be 5 years and 7 months. This is when the difference between the cumulative cash flow of the proposed system and the base case system turns negative to positive. The payback shows how long it would take to make up the investment cost difference between the proposed system and the existing one. This demonstrates unequivocally that the proposed system has a clear economical advantage over the existing energy system for the 25-year project life span.

6.2. Emission comparison

Gas emission from fossil fuel combustion has been recognized as a worldwide problem due to global warming and its associated effects. The comparison of CO2 emissions and other GHG gases of the base and proposed power system is presented in Fig. 18. The base case system created higher emissions than the proposed HRES for every pollutant considered. The high frequency of grid outages significantly increases the run time of the backup DG to meet energy demand in the base case, as shown in Fig. 19. From the results presented in Table 6, deploying the proposed HRES reduces the annual diesel fuel usage from 84,351 litres per year to 3110 litres per year. Therefore, decreasing the CO2 emission by 86%, the CO emission by 96%, sulphur dioxide by 81%, and nitrogen oxides by 58%. This is significate, considering the present amount of GHG emissions worldwide. Implementing systems like this will go a long way toward increasing energy and environmental sustainability.

7. Conclusion

This study focuses on HRES optimisation to demonstrate the viability of harnessing energy resources available on farms to reliably satisfy the farm environment's energy demands. An extensive analysis of an autonomous HRES comprising PV/WT/BG/BS/GD/DG was carried out. An economic dispatched strategy was developed to suit the peculiarity of the local energy status. A comparative analysis for optimal sizing of the HRES based on three popular metaheuristic algorithms, namely ABC, GA, and PSO algorithms, has been presented. The sizing of the HRES is performed to fully meet the energy demand of a dairy farm in north-central Nigeria without violating any of the predetermined constraints. PSO was determined to be the best-performed algorithm with a good balance between exploitation and exploration, attaining the lowest LCOE with the least amount of iteration. PSO algorithm was then compared with a popular commercially available (HOMER Pro) application. Finally, the proposed HRES was compared with the existing power system in the case study. The obtained results demonstrate that incorporating solar PV and BG into the existing power system can significantly reduce GHG emissions and affordably provide the long-term energy needs of developing countries.

Declaration of Competing Interest

The authors state that they have no known conflicting financial or personal interests that may have seemed to affect the work presented in this study.

Data availability

The authors do not have permission to share data.

References

[1] L. Olatomiwa, A.A. Sadiq, O.M. Longe, J.G. Ambafi, K.E. Jack, T.A. Abdulazeez, An overview of energy access solutions for rural healthcare facilities, Energies 12 (9554) (2022) 1–23, https://doi.org/10.3390/en15249554.

[2] World-bank, "Nigeria to improve electricity access and services to citizens", 2021. https://www.worldbank.org/en/news/press-release/2021/02/05/nigeria-to-improve-electricity-access-and-services-to-citizens (accessed Aug. 06, 2022).

[3] D. Akinyele, I. Okakwu, E. Olabode, R. Blanchard, T. Ajewole, Integrated TEEP approach to microgrid design and planning with small hydro /solar / diesel resources for standalone application, e-Prime Adv. Electr. Eng. Electron. Energy 2 (2022) 1–15, https://doi.org/10.1016/j.prime.2022.100091, no. Novemberpp.

[4] S.O. Sanni, J. Yakubu, T. Oluwafemi, Analysis of backup power supply for unreliable grid using hybrid solar PV /diesel / biogas system, Energy 227 (2021), 120506, https://doi.org/10.1016/j.energy.2021.120506.

[5] L. Olatomiwa, R. Blanchard, S. Mekhilef, D. Akinyele, Hybrid renewable energy supply for rural healthcare facilities : an approach to quality healthcare delivery, Sustain. Energy Technol. Assess. 30 (2018) 121–138, https://doi.org/10.1016/j.seta.2018.09.007, no. February.

[6] S. Singh, M. Singh, S. Chandra, Feasibility study of an islanded microgrid in rural area consisting of PV, wind, biomass and battery energy storage system, Energy Convers. Manag. 128 (2016) 178–190, https://doi.org/10.1016/j.enconman.2016.09.046.

[7] Q. Hassan, M. Jaszczur, A.K. Al-Jiboory, A.A. Hasan, Optimizing of hybrid renewable photovoltaic/wind turbine/super capacitor for improving self-sustainability, Energy Harvest. Syst. 9 (2) (2022) 151–164, https://doi.org/10.1515/ehs-2021-0095.

[8] Q. Hassan, M. Jaszczur, S.A. Hafedh, M.K. Abbas, A.M. Abdulateef, A. Hasan, Optimizing a microgrid photovoltaic-fuel cell energy system at the highest renewable fraction, Int. J. Hydrog. Energy 47 (42) (2022), https://doi.org/10.1016/j.ijhydene.2022.02.108.

[9] A. Bouaouda, Y. Sayouti, Hybrid Meta-Heuristic Algorithms for Optimal Sizing of Hybrid Renewable Energy System: A Review of the State-of-the-Art, Springer, Netherlands, 2022, https://doi.org/10.1007/s11831-022-09730-x no. 0123456789.

[10] D. Ribo-Perez, A. Herraiz-Canete, D. Alfonso-Solar, C. Vargas-salgado, T. Gomez-Navarro, Modelling biomass gasifiers in hybrid renewable energy microgrids ; a complete procedure for enabling gasifiers simulation in HOMER, Renew. Energy 174 (2021), https://doi.org/10.1016/j.renene.2021.04.083.

[11] L. Olatomiwa, S. Mekhilef, M.S. Ismail, M. Moghavvemi, Energy management strategies in hybrid renewable energy systems : a review, Renew. Sustain. Energy Rev. 62 (2016) 821–835, https://doi.org/10.1016/j.rser.2016.05.040.

[12] H. Hassanzadehfard, F. Tooryan, V. Dargahi, S. Jin, A cost-efficient sizing of grid-tied hybrid renewable energy system with different types of demands, Sustain. Cities Soc. 73 (2021), 103080, https://doi.org/10.1016/j.scs.2021.103080 no. June.

[13] S. Salisu, M. Wazir, L. Olatomiwa, Assessment of technical and economic feasibility for a hybrid PV-wind-diesel-battery energy system in a remote community of north central Nigeria, Alex. Eng. J. (2019), https://doi.org/10.1016/j.aej.2019.09.013.

[14] M. Kiehbadroudinezhad, A. Rajabipour, Modeling, design, and optimization of a cost-effective and reliable hybrid renewable energy system integrated with desalination using the division algorithm, Int. J. Energy Res. (2020) 1–24, https://doi.org/10.1002/er.5628, no. May.

[15] W. He, L. Tao, L. Han, Y. Sun, P. Elia, J. Yan, Optimal analysis of a hybrid renewable power system for a remote island, Renew. Energy 179 (2021) 96–104, https://doi.org/10.1016/j.renene.2021.07.034.

[16] H. Yang, W. Zhou, L. Lu, Z. Fang, Optimal sizing method for stand-alone hybrid solar – wind system with LPSP technology by using genetic algorithm, Sol. Energy 82 (2008) 354–367, https://doi.org/10.1016/j.solener.2007.08.005.

[17] Y. Ho, D.L. Pepyne, Simple explanation of the no free lunch theorem of optimization, in: Proceedings of the IEEE Conference on Dicision and Control, IEEE, 2001, pp. 1–6.

[18] M. Shara, T.Y. Elmekkawy, Multi-objective optimal design of hybrid renewable energy systems using PSO-simulation based approach, Renew. Energy 68 (2014) 67–79.

[19] O. Hazem, O. Hazem, Particle swarm optimization of a hybrid wind /tidal / PV / battery energy system application to a remote area in bretagne, cooling France energy system, A Energy Procedia 162 (2019) 87–96, https://doi.org/10.1016/j.egypro.2019.04.010.

[20] T.O. Ajewole, M.O. Omoigui, O.D. Ayedun, Optimal component configuration and capacity sizing of a mini integrated power supply system, Environ. Qual. Manag. (2019) 1–6, https://doi.org/10.1002/tqem.21639.

[21] M. Gharibi, A. Askarzadeh, Size and power exchange optimization of a grid-connected diesel generator-photovoltaic-fuel cell hybrid energy system considering reliability, cost and renewability, Int. J. Hydrog. Energy 44 (47) (2019) 25428–25441, https://doi.org/10.1016/j.ijhydene.2019.08.007.

[22] V. Ani, Optimal control of PV / Wind / hydro-diesel hybrid power generation system for off-grid Macro base transmitter station site, Electron. J. Energy Environ. 1 (2) (2017) 37–55, https://doi.org/10.7770/ejee-V1N2-art605.

[23] S.O. Sanni, M. Ibrahim, I. Mahmud, T. Oluwafemi, K.O. Olusuyi, Potential of off-grid solar PV /biogas power generation system : case study of ado ekiti slaughterhouse, Int. J. Renew. Energy Res. 9 (3) (2019) 1309–1318.

[24] A. Benjamin, A. Felix, O. Oghorada, K. Ogbeide, A.A. Awelewa, and A.E. Afolabi, "Reliability assessments of an islanded hybrid PV-diesel-battery system for a typical rural community in Nigeria", Heliyon, vol. 5, pp. 1-13, 2019, 10.1016/j.heliyon.2019.e01632.

[25] S.A. Adetoro, M.N. Nwohu, L. Olatomiwa, Techno-economic analysis of hybrid energy system connected to an unreliable grid : a case study of a rural community in Nigeria, in: Proceedings of the IEEE Nigeria 4th International Conference on Disruptive Technologies for Sustainable Development (NIGERCON), IEEE, 2022, pp. 1–5, https://doi.org/10.1109/NIGERCON54645, pp.2022.9803128 2022.

[26] M. Shaaban, J.O. Petinrin, Renewable energy potentials in Nigeria : meeting rural energy needs, Renew. Sustain. Energy Rev. 29 (2014) 72–84, https://doi.org/10.1016/j.rser.2013.08.078.

[27] "NASA/SSE", Surface meteorology and Solar Energy 2016. http://eosweb.larc.nasa.gov/sse, (accessed Oct. 09, 2022).

[28] S. Alsadi, T. Khatib, Photovoltaic power systems optimization research status: a review of criteria, constrains, models, techniques, and software tools, Appl. Sci. 8 (1761) (2018) 1–30, https://doi.org/10.3390/app8101761.

[29] M.R. Akhtari, M. Baneshi, Techno-economic assessment and optimization of a hybrid renewable co-supply of electricity, heat and hydrogen system to enhance performance by recovering excess electricity for a large energy consumer, Energy Convers. Manag 188 (2019) 131–141, https://doi.org/10.1016/j.enconman.2019.03.067. January.

[30] S.M. Dawoud, Developing different hybrid renewable sources of residential loads as a reliable method to realize energy sustainability q, Alex. Eng. J. 60 (2) (2021) 2435–2445, https://doi.org/10.1016/j.aej.2020.12.024.

[31] H. Abd El-Sattar, S. Kamel, H. Sultan, M. Tostado-Véliz, A.M. Eltamaly, F. Jurado, Performance analysis of a stand-alone pv/wt/biomass/bat system in alrashda village in egypt, Appl. Sci. 11 (21) (2021), https://doi.org/10.3390/app112110191.

[32] S. Jamshidi, K. Pourhossein, M. Asadi, Size estimation of wind /solar hybrid renewable energy systems without detailed wind and irradiation data : a feasibility study, Energy Convers. Manag. 234 (2021), 113905, https://doi.org/10.1016/j.enconman.2021.113905. March.

[33] V. Suresh, M. Muralidhar, R. Kiranmayi, Modelling and optimization of an off-grid hybrid renewable energy system for electrification in a rural areas, Energy Rep. 6 (2020) 594–604, https://doi.org/10.1016/j.egyr.2020.01.013.

[34] A. Honest, J. Saria, Performance of experimental bio-digestion for pathological and biodegradable waste management at mwananyamala regional referral hospital Tanzania, J. Environ. Prot. 11 (10) (2020) 838–847, https://doi.org/10.4236/jep.2020.1110052 (Irvine, Calif).

[35] A.L. Bukar, C.W. Tan, K.Y. Lau, Optimal sizing of an autonomous photovoltaic/wind/battery/diesel generator microgrid using grasshopper optimization algorithm, Sol. Energy 188 (2019) 685–696, https://doi.org/10.1016/j.solener.2019.06.050, no. May.

[36] R. Atia, N. Yamada, Optimization of a PV-wind-diesel system using a hybrid genetic algorithm, in: Proceedings of the IEEE Electrical Power and Energy Conference, IEEE, 2012, pp. 80–85.

[37] T.O. Ajewole, O. Oladepo, K.A. Hassan, A.A. Olawuyi, O. Onarinde, Comparative study of the performances of three metaheuristic algorithms in sizing hybrid-source power system, Turk. J. Electr. Power Energy Syst. 10 (2022) 1–13, https://doi.org/10.5152/tepes.2022.22012.

[38] L. Cioccolanti, R. Tascioni, R. Moradi, M. Pirro, C. Maria, I. Makhkamova, Development of a smart control unit for small-scale concentrated solar combined heat and power systems for residential applications, e-Prime Adv. Electr. Eng. Electron. Energy 2 (2022), https://doi.org/10.1016/j.prime.2022.100040 no. April.

[39] R. Bose, H. Mondal, I. Sarkar, S. Roy, Design of smart inventory management system for construction sector based on IoT and cloud computing, e-Prime Adv. Electr. Eng. Electron. Energy 2 (2022), 100051, https://doi.org/10.1016/j.prime.2022.100051. June.

[40] S.A. Adetoro, L. Olatomiwa, J. Tsado, S.M. Dauda, An overview of configurations and dispatch strategies in hybrid energy systems, in: Proceedings of the IEEE Nigeria 4th International Conference on Disruptive Technologies for Sustainable Development (NIGERCON), IEEE, 2022, pp. 10–15, https://doi.org/10.1109/NIGERCON54645.2022.9803082.

[41] A. Baruah, M. Basu, D. Amuley, Modeling of an autonomous hybrid renewable energy system for electrification of a township : a case study for Sikkim, India, Renew. Sustain. Energy Rev. 135 (2021), 110158, https://doi.org/10.1016/j.rser.2020.110158 no. July 2020.

[42] K. Anoune, M. Bouya, A. Astito, A. Ben, Sizing methods and optimization techniques for PV-wind based hybrid renewable energy system : a review, Renew. Sustain. Energy Rev. 93 (2018) 652–673, https://doi.org/10.1016/j.rser.2018.05.032, no. May.

[43] K. Sopian, A. Zaharim, Y. Ali, Z.M. Nopiah, J.A.B. Razak, N.O.R.S. Muhammad, Optimal operational strategy for hybrid renewable energy system using genetic algorithms, in: Proceedings of the 12th WSEAS International Conference on Applied Mathematics, Cairo, Egypt 7, WSEAS, 2008.

[44] M. Nemati, M. Braun, S. Tenbohlen, Optimization of unit commitment and economic dispatch in microgrids based on genetic algorithm and mixed integer linear programming, Appl. Energy (2017) 1–20, https://doi.org/10.1016/j.apenergy.2017.07.007.

[45] M. Amer, A. Namaane, N.K.M. Sirdi, Optimization of hybrid renewable energy systems (HRES) using PSO for cost reduction, Energy Procedia 42 (2013) 318–327, https://doi.org/10.1016/j.egypro.2013.11.032.

[46] M.A. Mohamed, A.M. Eltamaly, A.I. Alolah, PSO-based smart grid application for sizing and optimization of hybrid renewable energy systems, PLoS One 11 (8) (2016) 1–22, https://doi.org/10.1371/journal.pone.0159702.

Saheed Ayodeji Adetoro obtained his Bachelor's degree (B. Eng.) in Electrical and Computer Engineering from the Federal University of Technology, Minna and his Master's degree (M. Eng.) in Electrical-Power Engineering from the University of Technology Malaysia. Saheed is currently pursuing his PhD in Power System Engineering at the Federal University of Technology, Minna. His research interest is in the area of Renewable Energy Systems. He is a registered Engineer with the Council for the Regulation of Engineering in Nigeria (COREN). He is presently an academic staff at the Federal Polytechnic, Bida, Niger State.

Lanre Olatomiwa obtained B.Eng and M.Eng degree in Electrical Engineering/Electronics from Federal University of Technology Minna, Nigeria, and a PhD degree in Renewable Energy systems at University of Malaya, Malaysia. He is an Associate Professor of Electrical Engineering and is currently the Head of the Department of Electrical/Electronics Engineering Federal University of Technology, Minna. Nigeria. His research interests include; hybrid renewable energy systems, energy management in hybrid systems, Demand Side management, rural healthcare power development and optimization techniques for renewable energy (RE) integration. He has published extensively in high-impact Journals.

Jacob Tsado is a Professor of Electrical and Electronics Engineering in the Department of Electrical & Electronics Engineering, Federal University of Technology Minna. He obtained B.Eng in Electrical and Computer Engineering from the Federal University of Technology Minna and M.Eng and PhD degrees in Power System & Machine both from the University of Benin, Benin City Nigeria. He is a registered Engineer with the regulatory agency in Nigeria. He was Head of the Department of Computer Engineering and the immediate past Head of Electrical & Electronics Engineering Department Federal University of Technology, Minna. His research interests include; power system analysis, power system protection schemes and energy studies, he has published scholarly publications locally and internationally.

Solomon Musa Dauda is a Professor of Agricultural and Bioresources Engineering in the School of Infrastructure, Process Engineering and Technology, Federal University of Technology Minna. He holds a B.Eng. degree from the University of Maiduguri, Nigeria, M.Eng. degree from the Federal University of Technology Minna, Nigeria and a PhD from Universiti Putra Malaysia. He is the immediate past Acting Dean of the School of Infrastructure, Process Engineering and Technology and the current Head of the Department of Agricultural and Bioresources Engineering, Federal University of Technology Minna. His research interests are in the areas of Agricultural Power, Mechanization and Renewable energy. He has to his credit many scholarly publications.